# TOWARD JOINT WATER-POWER ELECTRIC GRID MODELING

BY

DESIREE PHILLIPS

DISSERTATION

Submitted in partial fulfillment of the requirements
for the degree of Doctor of Philosophy in Electrical and Computer Engineering
in the Graduate College of the
University of Illinois at Urbana-Champaign, 2018

Urbana, Illinois

Doctoral Committee:

Professor Thomas Overbye, Chair
Assistant Professor Subhonmesh Bose
Professor Peter Sauer
Assistant Professor Ashlynn Stillwell
Assistant Professor Hao Zhu

# ABSTRACT

The water-energy nexus refers to the relationship between how much water is used to generate and transmit energy, and how much energy it takes to collect, clean, move, store, and dispose of water. The dependence of the electric power grid on water varies based on generation technology (i.e., prime mover), fuel source, cooling technology, and climate. By one estimate, 49% of all U.S. water withdrawals are used for thermoelectric cooling, with the state of Illinois ranking second overall in terms of thermoelectric-cooling withdrawal.

This work proposes the introduction of water-dependency variables into existing electric grid analysis, specifically for the state of Illinois. The goal is to more explicitly examine how the changes in water use and availability affect electric grid operation and reliability. Collections of relevant electric grid and water data are publicly available, but minimal work has been done in combining these datasets for electric grid analysis.

A synthetic electric grid model of the state of Illinois was augmented with water parameters which quantify the interdependent nature of water and energy adequacy in terms of cost and reliability. Using Illinois climate data, reliability analysis was able to develop a probabilistic parameter that characterized a generator's potential for operating at a reduced capacity due to weather conditions. In addition, a cost parameter was developed by measuring the volume of water used for power plant cooling and the cost of water acquisition. This cost was added to the fuel cost of electricity in order to quantify, in terms of profits and bidding strategies, a power plant's dependence on cooling water availability.

# ACKNOWLEDGMENTS

Foremost, I would like to express my sincere gratitude to my advisor Prof. Thomas Overbye. His patience and enthusiasm were constants throughout my graduate years, and he allowed me the space to work in my own way. His guidance and motivation were invaluable; I could not imagine having a greater advisor.

My parents Carol and Kenneth and brother Vaughn have provided love and emotional support that have been constants throughout my life. I am also grateful to the other friends and family who have supported me in all my endeavors.

I want to thank the Institute for Sustainability, Energy, and Environment (ISEE) for funding this interdisciplinary research. A special thank you goes to William Lubega and Ashlynn Stillwell, civil engineers whose work significantly contributed to this dissertation.

Last but certainly not least, thanks to the power and energy systems students, staff, and faculty for making the University of Illinois at Urbana-Champaign feel like home. The six years spent here were made all the more fantastic because of the social and academic activities we took part in together.

# TABLE OF CONTENTS

# CHAPTER 1

# INTRODUCTION

## 1.1 Motivation

Water and energy systems are heavily intertwined. Producing energy requires water for cooling electric generators, and energy is needed for the treatment, extraction, and delivery of water used for various applications. This linkage means that changes and constraints in one sector can indirectly affect the function and reliability of the other. Despite this interdependency, the regulation and management of the water and energy systems are typically handled independently, both nationally and regionally.

### 1.1.1 Water Usage

Much like electricity, water does not directly flow to those who pay the highest price. As a result, the price for water-intensive users may not be all that different from minimal-water users, implying inefficient water usage. Water prices do not factor in the supply technique or treatment process, nor do they capture local water availability. Due to changes in the water-energy landscape driven by climate change and population growth, this more liberal usage of water is starting to change.

In recent years, climate change has resulted in measured increases in regional temperatures and decreased precipitation rates. These shifts in weather conditions have created critical reductions in water volume across many U.S. bodies of water, exacerbating existing water availability problems. California's severe drought conditions, for example, led to reductions in hydropower (which on average accounts for 14-19% of the states' electricity) that required natural gas and renewable generation to make up the difference [1].

### 1.1.2 Water-Energy Research

A number of technical reports assess the current and future projections of water stresses. In their 2011 report, the Electric Power Research Institute (EPRI) indicated a significant portion of the southern United States faces growing thermoelectric water stresses [2]. Additionally, the National Energy Technology Laboratory also examined water vulnerabilities of the United States' coal production [3].

In order to better understand the changes in the water-energy landscape, the Government Accountability Office (GAO) has released a series of reports calling for improved data collection and analysis. In 2009, they published a technical report proposing improved federal water data use in order to understand trends in power plant water use; another 2012 report outlined a coordinated federal approach needed to better manage energy and water tradeoffs [4, 5].

As a result of calls for data and analysis, research relating to the interdependency between water and energy has seen significant growth in the last few decades. Various federal agencies and national organizations, including the Department of Energy (DOE) and National Science Foundation (NSF), have provided funding opportunities and calls for proposals in order to address this water-energy nexus (WEN) [6, 7]. Various WEN agendas and meetings have highlighted common research demands and objectives, including:

- increased water and energy data collection,
- development of decision support tools that incorporate these data, and
- joint policy and regulation structures [8, 9, 10].

As the water and energy data collection improves, cross-sectional tools and analysis techniques need to be developed. This area of integrated design, research, and engineering has been identified by stakeholders and numerous research groups as a point of interest that currently lacks significant groundwork and exploration. Attendees of the 2015 DOE Water-Energy Nexus Roundtable Series stated:

> Water resources can significantly affect reliability and resilience of energy systems at local, regional, and national scales. A consideration of risk related to water should therefore be embedded

into energy systems analysis, design, planning, business models, and technology employment [11].

In one of the most comprehensive water-energy reports for the United States, *The Water-Energy Nexus: Challenges and Opportunities*, the DOE outlines state roles within the water-energy nexus, data modeling and analysis priorities, and potential R&D opportunities [12]. While many of the current models have focused on geographical analysis, human systems, and their interactions, the report cited a need for characterization of uncertainty and risks as well as robust analyses at decision-relevant scales. With climate change, more accurate models will be needed because "energy and water systems are generally adapted to existing climate... [and] changes will almost always require some costly adjustment".

## 1.2 Outline

In an effort to address the need for interconnected water-energy analysis, this research augments existing power system modeling and analysis techniques with water-dependent variables and parameters. The power systems areas to be addressed in this work are electricity markets and system reliability, with electric generation planning introduced as well.

Due to the demographic changes in water use and availability, along with the state-level regulation of water usage, the proposed work will be applied to a state-level power system model. The state to be analyzed is Illinois, and the electric grid model is fictitious, developed using a combination of power system statistics, regulatory parameters, and publicly available electricity data.

### 1.2.1 Power System Reliability

Traditional power system reliability metrics such as forced outage rate have not explicitly considered the effects of cooling water supply. However, as water stresses continue to grow, competition between water users may result in additional instances of reduced generation capacity. In *Texas Commission on Environmental Quality (TCEQ) v. Texas Farm Bureau*, Texas courts

ruled that the TCEQ did not have the authority, in the event of a drought, to prioritize thermoelectric generation over other water users [13, 14, 15]. In such a case, the electric grid will have to deal with the possibility of curtailments and/or shutdowns.

To address this potential for curtailments, the reliability analysis introduces a water-based derating capacity and probability into generation adequacy assessment. Temperature and streamflow statistics are used to develop the derating parameters that determine the effects of drought and/or heatwaves on system reliability. With these new parameters, Monte Carlo methods are used to determine the effect of derating events on system capacity and reliability projections.

### 1.2.2 Electricity Market

In Australia and the state of California, water-constraints have created situations of increased water competition. The uncertainty around water supply has motivated the move from long-term water contracts to volume-based payment for only the water used [16]. This short-term payment manifests itself in the form of water markets and water trading in order to more efficiently use existing water resources.

In the event that similar water management tactics become more common in water-stressed regions of the United States, the price that the buyer has to pay for water may affect the cost efficiency of a utility's generation units. The electricity market work proposes a water cost parameter that can provide insight into the ways in which water limitations could drive the price of electricity. The purpose of the analysis is to:

1. Determine an effective water cost that explicitly quantifies a plant configuration's dependence upon water,

2. Examine how this parameter changes unit commitments operating costs, and

3. Analyze changes in profits and asset valuation given a unit's dependence on cooling water availability.

# CHAPTER 2

# WATER FOR ELECTRICITY

## 2.1 Thermoelectric Cooling

Thermoelectric power refers to electricity generated from a heat source with the help of a prime mover, a medium that converts fuel into the mechanical energy required by an electric generator [17]. The generator then converts the input mechanical (rotational) energy into the electrical output that is fed to the power grid.

Thermoelectric technologies differ in fuel source (e.g., fossil fuel, nuclear, geothermal), cooling technology (e.g., open-loop, closed-loop, dry), and prime mover (e.g., steam turbine, gas combustion turbine). The amount of water needed for thermoelectric cooling is directly correlated with the power plant configuration (i.e., prime mover, fuel, and cooling combination). Typically, coal plants have the lowest energy efficiencies but second highest water usage [18].

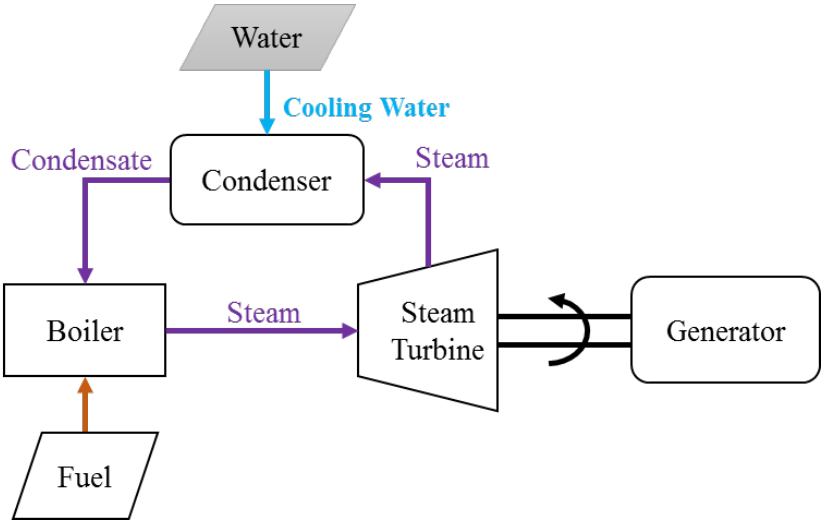


Figure 2.1: General view of the thermoelectric generation cycle.

Figure 2.1 provides a broad view of a thermoelectric generator. In this case the prime mover is the steam turbine; cooling takes place in the condenser. Electricity generation begins in the boiler, where *feedwater* is turned into steam using a fuel-driven combustion or heating process. The steam is then used to drive the prime mover (i.e.: steam turbine). Cooling water, indicated by the gray parallelogram in Fig. 2.1, is needed in order to condense the feedwater so that it may be re-used in the next boiler cycle.

The feedwater is technically an additional source of water used by the generator. Water's high specific heat capacity allows it to capture significant amounts of thermal energy (used to drive the prime mover) without a large change in temperature [19]. For the purposes of this work, however, it is neglected because it is separate from the cooling water.

Water usage for thermoelectric cooling accounts for almost 50% of the daily water withdrawals within the U.S. and can be broken down into consumed and withdrawn water [12]. Withdrawn water is taken from a body of water (e.g., ocean, lake, river) for the purpose of cooling, while consumed water is lost to evaporation during cooling [20].

Of the currently available cooling technologies, the two most commonly used are of the open-loop (e.g., "once-through") and closed-loop (e.g., "re-circulating") varieties. Together, these two technologies make up approximately 68% of water withdrawals, 67% of water consumption, and 52% of the net electricity generation within the United States [21].

### 2.1.1 Open-Loop Cooling

Traditionally, thermoelectric cooling within the United States significantly relied upon once-through technologies to condense the feedwater. With state and federal regulation, along with water scarcity issues exacerbated by population growth, the introduction of less water-dependent cooling technologies and the retirement of once-through generation units has been encouraged [21]. However, once-through cooling plants are still prevalent in the U.S., accounting for 23% of all electricity generated.

Figure 2.2 visualizes the open-loop cooling process. Cooling water is withdrawn from a nearby body of water and passed through a heat exchanger, cooling the steam so that it may be used in the next boiler cycle. While some

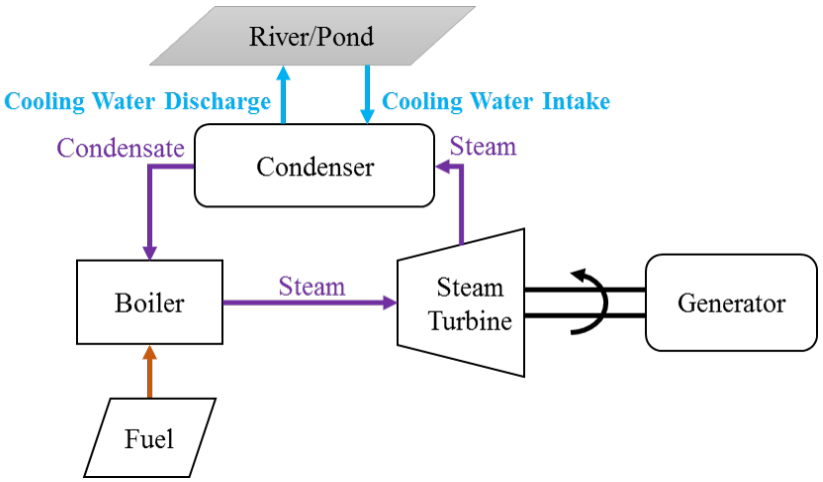


Figure 2.2: Open-loop cooling cycle.

water is lost to evaporation in the cooling process, the water withdrawals are orders of magnitude larger.

### 2.1.2 Closed-Loop Cooling

Due to the simultaneous retiring of open-loop units and introduction of alternative cooling technologies, closed-loop schemes have grown to become the primarily-used cooling technology, accounting for 29% of the U.S.'s net electricity generation. Figure 2.3 shows how most of the newer power plant installations are of the recirculating variety [21].

The closed-loop cooling process is demonstrated in Fig. 2.4. The recirculating refers to the reuse of a significant portion of the cooling water, which is cooled down for the next cycle within the cooling tower. To facilitate its shedding of the heat, a portion of the cooling water evaporates within the cooling tower and is replenished by withdrawing from a nearby body of water.

The use of the cooling tower allows for recycling of the cooling water, reducing system withdrawals significantly. However, consumption grows due to the evaporation that occurs within the tower.

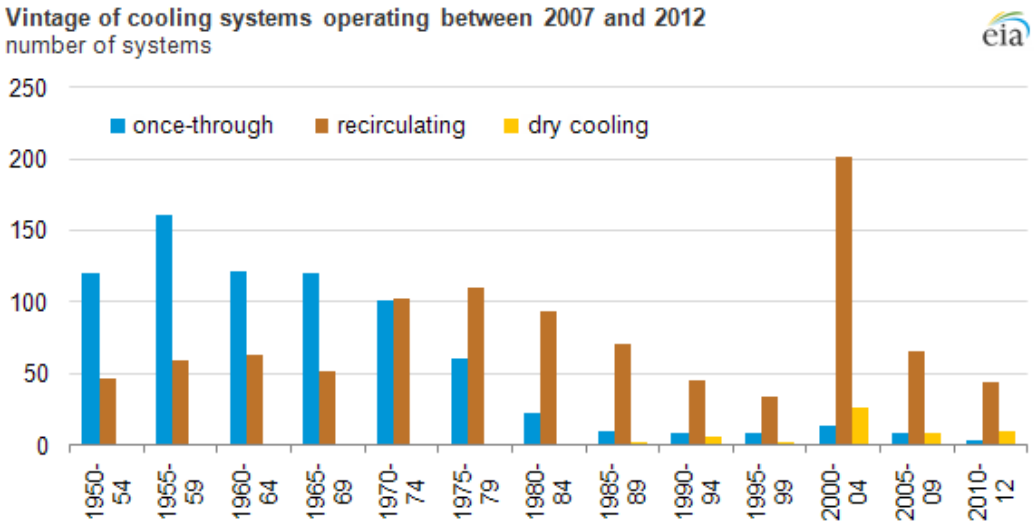


Figure 2.3: Recirculating technologies make up most of the newer plant cooling systems.

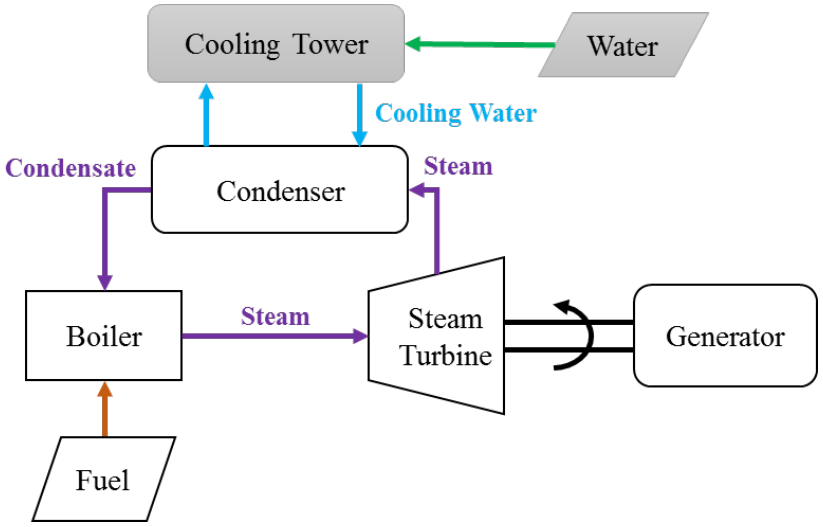


Figure 2.4: Closed-loop cooling via cooling tower.

## 2.2 Hydropower

Hydropower accounts for approximately 44% of the United States' renewable generation and 6.5% of overall power generation [22]. The DOE cited increasing temperatures, evaporative losses, precipitation changes, and decreasing snowpacks as the largest constraints on hydropower operation and available capacity [23].

The process can be explained using the graphic of Fig. 2.5. Water, through precipitation and melting of snow, collects in the hydroplant's reservoir: the

more water collected, the more hydropower that is available. As this water goes from the reservoir to the turbine, the potential energy contained in the change of elevation is used to drive the lower-elevation turbine, producing electricity.

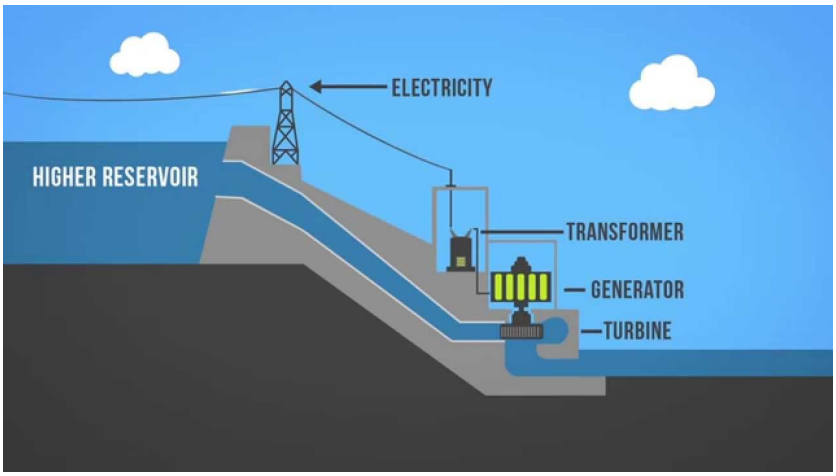


Figure 2.5: Cross-section of a hydropower plant.

Although hydropower does use significant amounts of water, as this is not cooling water, the water-dependencies of these units are not considered.

## 2.3 Regulation for Environmental Protection

### 2.3.1 Effluent Regulation

Power plants, in particular steam engines, may pollute the cooling water due to their method of water treatment, ash handling, and air pollution control [24]. Known as effluent, the makeup of this water can have negative impacts on the aquatic ecosystems as it is discharged from the plant after cooling. The Environmental Protection Agency (EPA), through its Clean Water Act (CWA), specifies the allowable temperature and pollution of this effluent for environmental protection [25]. Dependent upon stream conditions, this limit may be violated; Table 2.1 shows recorded effluent violations for IL power plants [26]; power plants whose cooling technology could not be identified are listed as "N/A".

Table 2.1: Power Plant Effluent Violations in Illinois

| **Plant Name** | **Fuel** | **Cooling** | **Date** | **Water Source** |
|---|---|---|---|---|
| Prairie State Generating Station | Coal | N/A | 12/31/2015 | Kaskaskia River |
| Quad Cities | Nuclear | Once-Through | 8/31/13-9/30/14 | Mississippi River |
| Mallard Lake Electric | Landfill Gas | N/A | 2/28/14 | Municipality |
| Calumet | Natural Gas | N/A | 12/31/2015 | Calumet River |

### 2.3.2 Water-Related Curtailments

When weather reduces streamflow and increases stream temperature, power plants may be given limited temperature-violation allowances known as *thermal variances* (TV). In 2012, for example, the Illinois EPA granted short-term thermal variances to multiple power plants that demonstrated sufficient need [27]. The following year, the Millstone Nuclear Power Station in Connecticut had to apply for an operating license amendment that increased their intake temperature limit from 75°F to 80°F [28]. Water-related curtailments and shutdowns for IL power plants are shown in Table 2.2 [26].

## 2.4 Water Usage Rights Within the U.S.

Within the United States, water usage rights developed based upon availability of water, with key legal doctrines developed in response to the water disputes and evolution in technology and usage. The distribution of these doctrines within the United States is shown in Fig. 2.6 [12].

Table 2.2: Water-Related Power Plant Curtailments in Illinois

| **EIA Name** | **Fuel** | **Cooling** | **Date** | **Reason** | **Resolution** |
|---|---|---|---|---|---|
| LaSalle Generating Station | Nuclear | Cooling Pond | 2001<br>2002<br>2005<br>2009<br>2010 | Intake/discharge water temperature | Followed extreme heat implementation plan |
| Dresden Generating Station | Nuclear | Cooling Pond | 2006 | Intake/discharge water temperature | Reduced Capacity |
| Will County | Coal | Once-Through | 2012 | Discharge water temperature | IL EPA attempted thermal variance |
| Joliet 9 | Coal | Once-Through | 2012 | Discharge water temperature | IL EPA attempted thermal variance |
| Joliet 29 | Coal | Once-Through | 2012 | Discharge water temperature | IL EPA attempted thermal variance |
| Quad Cities Generating Station | Nuclear | Once-Through | 2006 | Discharge water temperature | Curtailment; eventual shutdown |
| Powerton | Coal | Cooling Pond | 2012 | Discharge water temperature | Power output derated |
| Braidwood Generation Station | Nuclear | Cooling Pond | 2012 | Discharge water temperature | 102 °F variance offered |

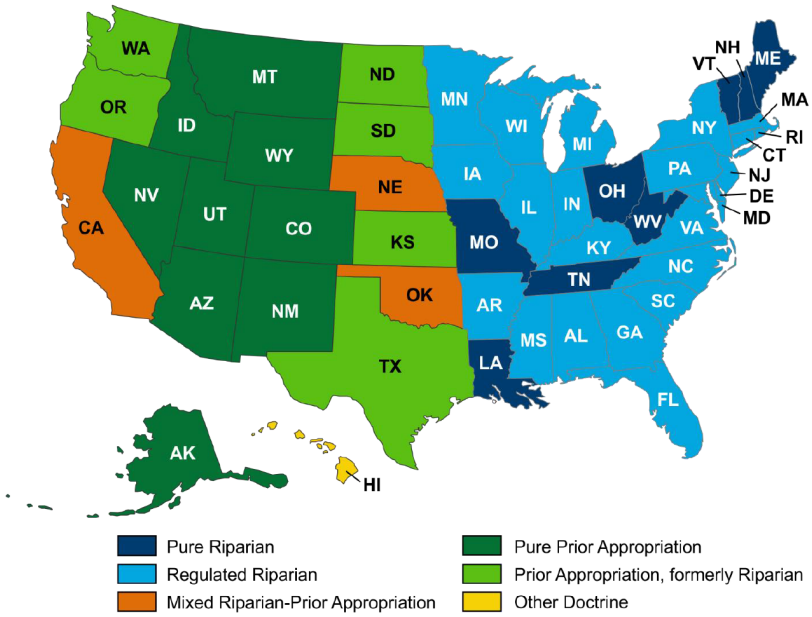


Figure 2.6: Water usage doctrines across the U.S.

### 2.4.1 Prior Appropriation, Riparian and Variations

Riparian rights evolved out of a dispute between mill owners over the use of river flow to generate mill power. The results of *Tyler v. Wilkinson*, the 1827 case in question, stated that all riparians have equal rights to the water flow from the river [29]. The upper proprietor has to make "reasonable use" of the water, and it cannot unreasonably divert or detain water so that the downstream proprietor has an unmitigated quantity of water flow. In the case of droughts and water scarcity, all riparian proprietors must share equally in the water shortage.

Riparian rights are with respect to land that is in contact with lakes and/or rivers, and in this way is tied to the land ownership. When this land is sold, the rights to the water are also transferred to the new owner. Whether this new owner continues to use the water or not, his rights to the water are not lost [30].

In the western U.S. where water is relatively scarce, and in response to the California gold rush, prior appropriation rights developed [31]. Unlike riparian rights, which are with respect to the owner of the adjacent land, prior appropriation rights are "first in time, first in right". The first person

to take water from a water source for "beneficial use" is then able to continue to use that water; the user of this water does not have to own the adjacent land.

There are additional constraints on this water usage, driven by scarcity and encapsulated within four essential elements of the doctrine:

- **Intent:** Appropriators have to demonstrate that they intend to use the water, within a given time frame, for a beneficial use.
- **Diversion:** A physical diversion of water from its source for applicable uses.
- **Beneficial Use:** A water use that is recognized and protected by law.
- **Priority:** Future ("junior") users of the same water source can only use water that does not infringe upon an earlier ("senior") appropriator's water usage [32].

In contrast to riparian rights, prior appropriation rights depend on the continued use of the water and can be lost through non-use. If desired, they can even be sold or traded. Regardless of appropriator, if changes in any aspect of the water usage (time/place/purpose of use, diversion point) would infringe upon the rights of another appropriator, the aggrieved appropriator can reject the changes.

### 2.4.2 Securing Water Rights for Power

Regardless of the intent of the water diverted, as long as it falls under "beneficial use", a new proprietor may submit a permit in an attempt to obtain water usage rights. While the exact definition of beneficial use varies from state to state, power generation and irrigation are commonly considered beneficial. However, whether new power plants can obtain these rights depends on additional factors, and these factors can become hurdles in the construction of a plant that requires water.

In Utah, a proposed nuclear plant being developed submitted an application in order to use the nearby Green River for its cooling. In order to be approved, a state engineer has to believe:

1. There was sufficient water available.

2. The proposed use did not infringe upon existing water usage.

3. The plant was physically and economically viable.

4. The project was not detrimental to public welfare.

5. The applicant could afford to complete the project.

6. The application was filed in good faith.

After two years of inspection by a state engineer it was determined that the plant met all of the state's requirements, and the water rights were secured for the plant [33]. When an appeal was submitted citing concerns relating to interference with existing use, over-appropriation of river water, and aquatic endangerment, the courts in *HEAL Utah v. Kane County Water Conservancy District* determined the permit was properly approved [34].

While some states moved completely to a prior appropriation doctrine in order to minimize water waste, other states have only partially introduced prior appropriation rights. These hybrid states allow riparian proprietors, in some instances, to claim seniority over prior appropriation users, given their doctrine existed first within the state. However, these rights are not recognized unless the riparian landowner claims their rights by a state-determined date [12, 32].

## 2.5 Existing Water-Electricity Models

This is not the first work to evaluate the water aspects of power generation in this manner. Researchers in [35] use a Rankine steam cycle to show how water temperature and availability affect the power and efficiency of steam plants. The National Renewable Energy Laboratory (NREL) developed a model that incorporates water and air temperature into electricity generation in order to determine water availability's effect on dispatch decisions in the Eastern U.S. [36]. Their model used climate to determine power plant thermal efficiencies, which were then input into an electricity model to determine the system performance and curtailments.

Argonne National Laboratory is one of the research laboratories endeavoring to fill the water-electricity gap with models and information. Along

with developing a tool that estimates water use, they have also analyzed drought impacts within the United States' Western and Texas Interconnections [37, 38]. The drought scenarios they developed quantify the weather-related risk to electricity generation. Through the use of drought parameters, they aimed to explicitly represent the effects of drought on available generation. In their future work, they cited a need for incorporation of economic impacts, drought duration, and climate change at the plant-level.

Several studies have analyzed the economic aspects of water usage for power generation via a water-based cost parameter. The work done in [39] developed a *$/MWh* water valuation parameter for Vietnam's major hydro reservoirs, applying it to the development of bidding strategies in a competitive market. A marginal cost of water was provided in [40, 41], created by retrofitting open-loop thermoelectric plants with either recirculating towers or dry cooling. The authors in [42] combined water intensities with electricity sales to determine the value intensity of water in the Western U.S. The valuation showed that water-trading between states implicitly existed due to the trading of electricity, and the study quantified this cost in in $/gal.

Unlike previous research, the models in this work focus on the usage of water for thermoelectric cooling. Using a similar cost parameter, changes in generation profits and asset valuation are determined in times of drought and water stress. Plant-level models are used to determine a steam plant's potential for derating based on fuel source and cooling technology. In addition to the climate constraints used by others, the plant model used in the reliability work incorporates regulation-driven water constraints such as the CWA.

This research furthers the work of researchers who developed water-cost parameters by applying them to a synthetic, fictitious model of the state of Illinois. In this way statistics, publicly-available generator data, and economic data for the state can be incorporated directly into the modeling and analysis.

# CHAPTER 3

# METHODOLOGY

## 3.1 Illinois Synthetic Network

Since water rights policies vary by state, it was desirable to have a state-level electric grid model for this analysis. The electric grid, however, is a United States critical infrastructure, so system information is of a proprietary nature. Of the publicly available test cases, equivalencing has reduced system complexity/accuracy or the network does not contain the type of data needed for a specified test case.

To address this issue, several research groups have looked into the development of synthetic, entirely fictitious electric grid models [43, 44, 45]. In particular, [46] showed the development of a synthetic ERCOT model for energy economic studies. It is this methodology that was used to create a 200-substation synthetic representation of the state of Illinois, referred to herein as the IL-200. Characteristics of the synthetic network are available in Table 3.1, and a one-line diagram shown in Fig. 3.1; the orange and black lines are 169 kV and 500 kV transmission lines, respectively. Economic analysis performed in [47] is outlined in the following sections and compared to actual Illinois economic data.

Table 3.1: IL-200 Characteristics

| | |
|---|---|
| Buses | 452 |
| Lines | 641 |
| Generators | 202 |
| Gen. Capacity | 50.6 GW |
| Total Load | 25.7 GW |

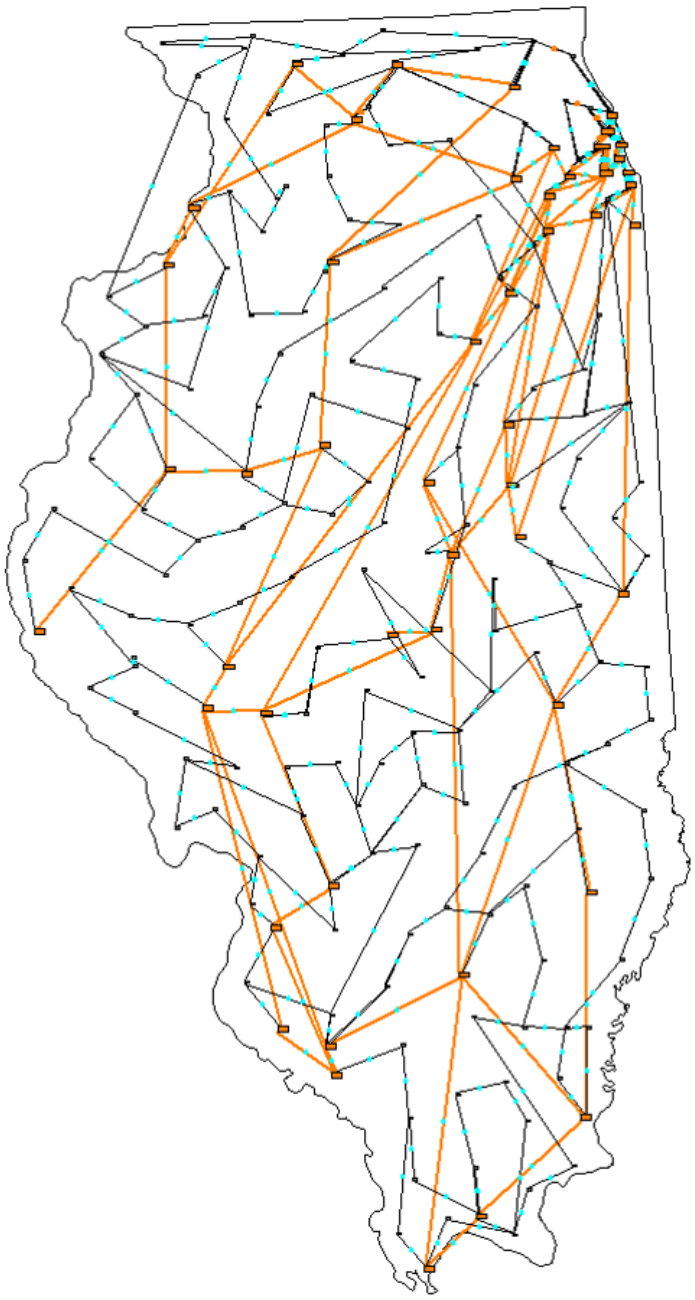

Figure 3.1: One-line diagram of the IL-200 synthetic network.

### 3.1.1 Economic Assessment

The supply curve of the IL-200 case is shown in Fig. 3.2; as expected, it is monotonically increasing. In assigning the quadratic cost functions for each of the generating units using statistical data, many of the values were close or overlapped. In aggregating these individual cost curves to create the system

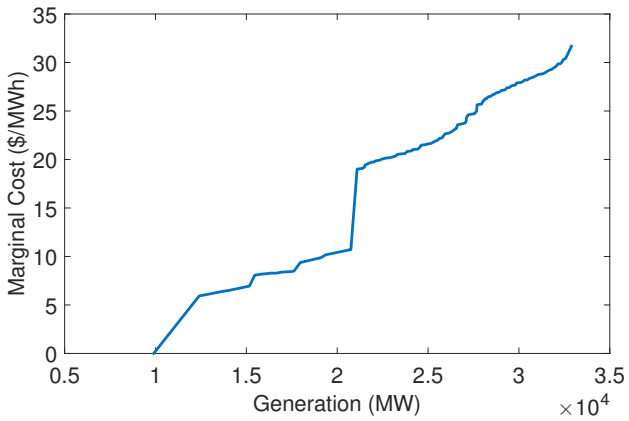


Figure 3.2: Supply curve of the IL-200 case.

supply curve, these values result in discrete continuities and sharp rises in cost [48].

To look at the feasibility of the synthetic economic results, the locational marginal prices (LMPs) are calculated at each bus using the Optimal Power Flow (OPF). Figure 3.3 shows the LMPs of the IL200 network when solved using the AC and DC OPFs. Not only are the shapes of their waveforms similar to one another, they are comparable to what is typically seen in the OPF literature as well [49]. The asymptotic behavior is seen in the ends of the AC LMP curve.

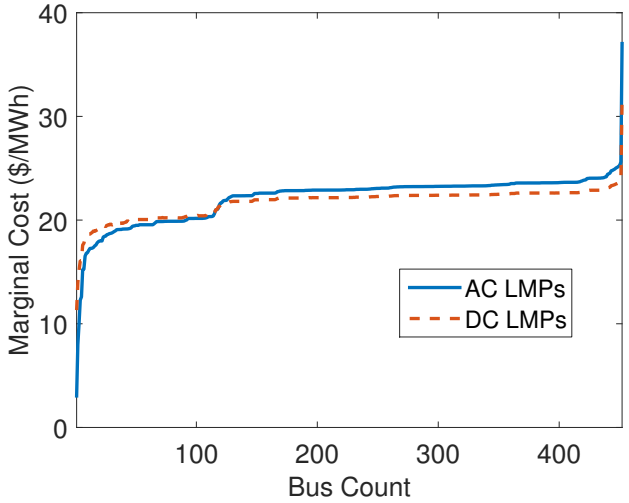


Figure 3.3: Comparison of the IL-200's LMPs using the AC and DC power flow.

### 3.1.2 Comparison to MISO Data

The LMP statistics for the IL-200 case using both AC and DC power flows (PF) are compared to the Midcontinent Independent System Operator (MISO) data for Illinois [50] in Table 3.2. As shown in Fig. 3.4, while there are fewer MISO data points to work with, the IL-200's LMP discontinuity also occurs in MISO's Illinois data.

Table 3.2: OPF Locational Marginal Price Statistics

| Measure | AC PF | DC PF | MISO |
|---|---|---|---|
| Mean ($/MWh) | 22.11 | 21.69 | 26.67 |
| S.Deviation ($/MWh) | 2.42 | 1.46 | 2.29 |

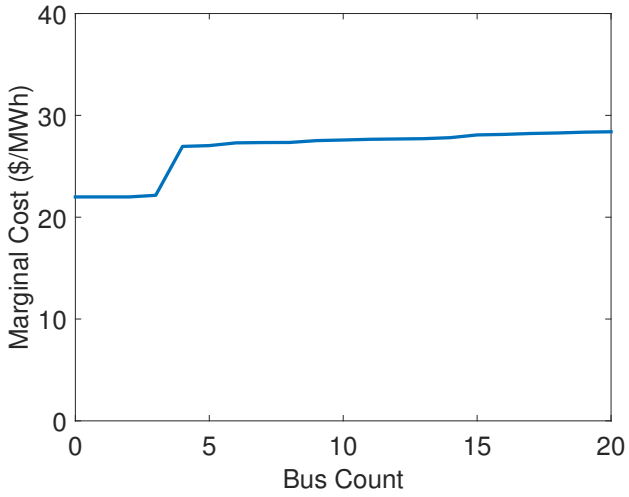


Figure 3.4: Distribution of the MISO LMPs in Illinois [50].

## 3.2 Water and Energy Data

Introduction of water parameters into the electric grid model requires the manipulation of water and electricity data from various sources.

One of the most comprehensive overviews of water use in the US comes from the United States Geological Survey's (USGS) *Estimated Use of Water in the United States* [51]. It provides breakdowns of water use by source (e.g. freshwater), sector of use (e.g., irrigation, thermoelectric power), and state (county resolution). This report is released every 5 years in cooperation

with state, federal, and local agencies, with the most recent publication a compilation of 2010 water use data, published in 2014.

On the electricity side, the Energy Information Administration (EIA) provides data on electricity sales, power plant technologies, fuel consumption, and water usage factors for generation plants larger than 1 MW. This collection is done using *Form EIA-860: Annual Electric Generator Report* and *Form EIA-923: Power Plant Operations Report* [52, 53].

Annual generator-level data about planned installations and retirements, divided by energy source, can be found in Form EIA-680. Water-related generator data includes the cooling technology (e.g., once-through, recirculating, hybrid, dry), intake water source (e.g., ground, surface, seawater), and water type (e.g., fresh, saline).

Form EIA-923 collects monthly and annual data on fuel consumption, fuel costs, and generation at the prime mover and power plant level. The status and water usage of cooling technologies for plants with a nameplate capacity of at least 10 MW is also provided. The withdrawal, diversion, discharge and consumption of cooling water, as well as estimated monthly cooling water consumption and temperatures, comprise the cooling information collected.

To help fill in the gaps on cooling data for the generation units who do not meet the 10 MW requirement, data compiled by the National Renewable Energy Laboratory (NREL) are used. Titled *A Review of Operational Water Consumption and Withdrawal Factors for Electricity Generating Technologies*, their literature review compiles estimates on water usage factors based on power plant technologies [54]; the full table of water factors is available in Appendix A.

# CHAPTER 4

# GENERATION ADEQUACY ASSESSMENT

## 4.1 Overview

Resilience and reliability studies have been evolving due to growing system complexity and regulation changes driven by environmental concerns. Intermittent sources such as wind and solar change the generation makeup of the grid; however, these sources of energy require generation availability that can account for their daily/hourly fluctuations. Additionally, drought and water uncertainty in water-stressed regions of the country have the potential to affect the flexibility of power plants that rely upon water for cooling.

In their report, the GAO indicated a growing number of states (40 of 50 as of 2013) are expecting water shortages in the next decade. Steps taken to improve water efficiency include the development of drought preparedness plans, water management tools, and conservation actions. As shown in Fig. 4.1, Illinois is expecting regional-level water shortages along with 24 other states [55].

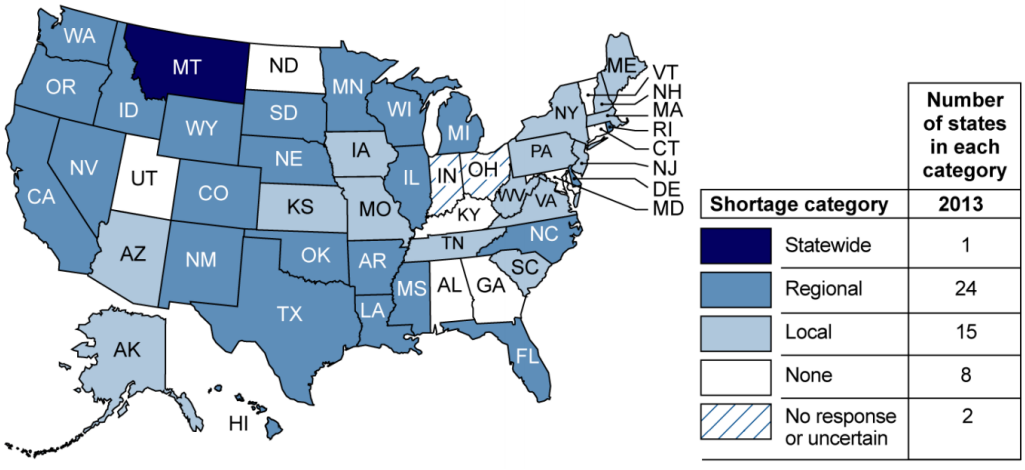


Figure 4.1: Predicted extent of state water shortages, 2013-2023 [55].

In order to capture water resource uncertainties, quantitative reliability analysis can be used to provide accurate metrics and risk factors. These factors should capture the water-uncertainty cited by the DOE, GAO, utilities, etc., so as to provide an accurate picture of the role water plays in power system operation and reliability.

This chapter introduces a water-based derating parameter that can be added to traditional power system reliability algorithms. Using a drought model developed by civil engineers at UIUC, water availability can be directly related to a generator's maximum capacity. With the relation quantified, the effects of droughts and heat waves can more directly be analyzed.

## 4.2 Generation Adequacy

While the exact definition of reliability may vary based upon the ultimate goal of the analysis, the typically used definition is the probability that an item will perform a required function for a given period of time. It can be broken down into adequacy and security aspects, the difference being whether the goal is to evaluate static or dynamic operation. Security focuses on transient stability and disturbance response, and adequacy relates to the existence of sufficient generation for the purpose of meeting system demand or operational requirements [56].

Within the realm of adequacy assessment, a significant portion of the reliability evaluation techniques are probabilistic rather than deterministic. Probabilistic methods have the advantage of including the likelihood of an event happening, not just the deterministic event severity or system impact. The stochastic nature of components, consumers, and grid behavior can be captured and quantified. This allows utilities and planners to determine where to allocate funds in order to improve system reliability in the long-term, as well as gauge the current system's resiliency.

In reliability analysis, it is useful to divide the overall electric grid into role-related segments. These "functional zones" are characterized using the three hierarchical levels outlined in [57] and shown in Fig. 4.2. The focus of Hierarchical Level 1 (HLI) is the ability of generation systems to meet system demand. Hierarchical Level 2 (HL2) examines the combined functionality of the generation and transmission systems, and Hierarchical Level 3 (HL3)

evaluates the consumer load point accuracy.

Given that water usage heavily influences generation availability, this reliability analysis will specifically look into developing water parameters for HL1: generation system adequacy.

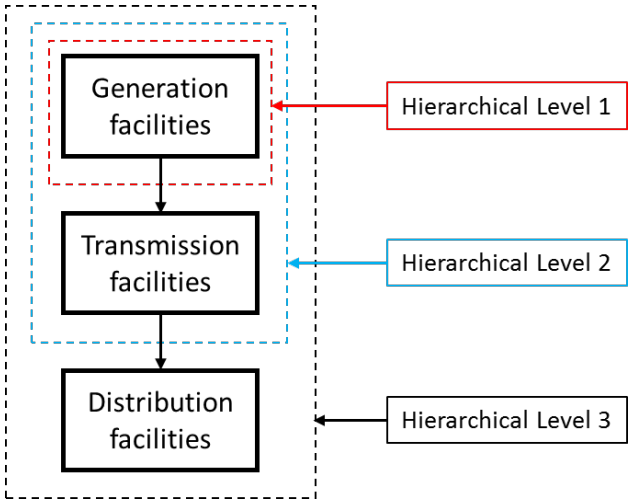


Figure 4.2: Hierarchical levels used in reliability evaluation.

Traditionally, the primary technique used in HL1 studies was a percentage reserve approach that, as its name implies, required a fixed percentage of the load or installed capacity to be available as system reserve. These methods have largely been replaced by probabilistic and stochastic techniques, allowing for system evolution to be factored in.

## 4.3 Monte Carlo Methods

One approach used for the stochastic analysis of power system reliability involves Monte Carlo methods. Using random numbers, created in part through component function/behaviors, the evolution of a power system is simulated over time. This experiment is performed numerous times in order to calculate the expected value of system reliability metrics.

The ability of Monte Carlo techniques to obtain accurate reliability metrics is based upon the law of large numbers (LLN):

$$\bar{X_n} = \frac{1}{n}\left(X_1 + X_2 + \cdots + X_n\right) \tag{4.1}$$

For a system in which reliability index $X$ is

$$\bar{X_n} \to \mu \quad \text{for} \quad n \to \infty \tag{4.2}$$

the sampled expectation will converge to the theoretical expectation.

As long as a sufficient number of simulations is performed, the measured reliability metrics should be approximately equal to the theoretical values, giving insight to the resiliency of the system being modeled.

### 4.3.1 State Sampling Method

The methods used in adequacy simulations primarily vary in computational complexity and the depth of generator data required. Preliminary work used the *state sampling method*, which has the following advantages over its counterparts [57]:

- For large-scale systems, the memory and computational burdens are smaller.
- Transition rates for generators are not required; only the state probabilities, which are typically easier to come by, are required.
- The state sampling method can more easily be extended to include additional weather and hydrological states [58].

For this methodology, each generator's behavior can be represented by a random number $U_i$ drawn from the uniform distribution $[0, 1]$. These generators are assumed to have up, down, and derated states; $U_i$ is used to determine unit $i$'s state for each simulation $k$:

$$S_i = \begin{cases} 1 & \text{(on)} & \text{if } U_i \geq \delta_i + \lambda_i \\ 2 & \text{(derated)} & \text{if } \lambda_i \leq U_i < \lambda_i + \delta_i \\ 0 & \text{(off)} & \text{if } 0 \leq U_i < \lambda_i \end{cases} \tag{4.3}$$

where $\lambda_i$ is the unit's forced unavailability and $\delta_i$ the probability of derating [59]. Whereas the on and off-state probabilities depend upon the expected forced unavailability of the unit, the derating probability is based on the cooling water availability.

Once the generators (and their operating histories) are converted into probabilistic variables, the total system capacity can be found. Using the forced unavailability and derating rate, state $S_i$ can be calculated for each unit. The total system capacity is then the sum of these units' capacities, calculated based upon their state.

Comparing the system capacity to the corresponding load indicates regions where the demand is greater than the capacity. Mathematically, this demand not served (DNS) for a system of $n$ units can be calculated using (4.4) [59]:

$$DNS_k = max\left\{0, D - \sum_{i=1}^{n} G_{ik}\right\} \tag{4.4}$$

where $D$ is the system demand and $G_{ik}$ is the capacity of unit $i$ in the $k$th sampling.

### 4.3.2 State Duration Sampling Method

As weather can be said to be chronological in nature, a sequential method is desired for large-scale system modeling. The *state duration sampling method* addresses this chronological nature by adding not only the duration between events, but the duration of the event itself. This method is arguably more popular than the state sampling method, which assumes independence between system states [56].

Rather than sampling states from predefined distributions, the duration of each state is sampled using the average lengths of operating, derating, and failing. As a result, the state duration sampling method requires additional information beyond what is required for the state sampling method. A state-space model is used to determine the components states and the likelihood of transitioning between them.

The two-state model for a base-load unit is shown in Fig. 4.3. It is the simplest representation of a unit, as it has only online (up) and offline (down) states. The likelihood of moving from one state to another depends on the mean time to failure (MTTF) and the mean time to repair (MTTR). Whereas the MTTF looks at the average length of time an object is expected to operate (i.e., how long before moving to the down state), the MTTR represents the unit's average repair time (i.e., how long before moving to the up state).

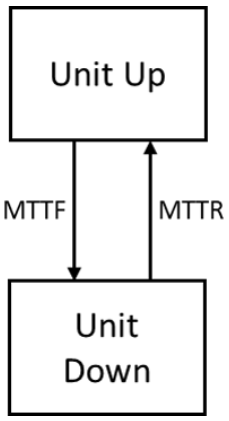


Figure 4.3: Two-state model for a base-load unit.

Since there is a desire to include a water-dependent derated state, the three-state model of Fig. 4.4 will be used. Along with the MTTF and MTTR parameters, the mean time to derating (MTTD) and mean derating duration (MDD) are needed to determine transitions to and from the derated state, respectively. These durations are dependent on weather conditions and cooling water availability, forces external to the generating unit.

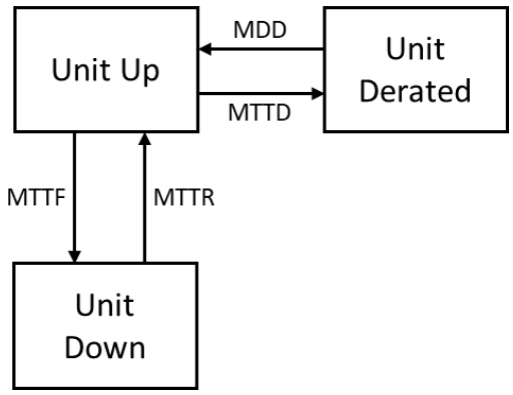


Figure 4.4: Three-state model for a base load unit.

Once the mean state durations are calculated, the length of time a unit will remain in a given state is obtained by sampling uniformly distributed

variables $U_i$:

$$TTF_k = -MTTF * \ln(U_1) \tag{4.5a}$$

$$TTD_k = -MTTD * \ln(U_3) \tag{4.5b}$$

$$TTR_k = -MTTR * \ln(U_2) \tag{4.5c}$$

$$DD_k = -MDD * \ln(U_4) \tag{4.5d}$$

For each iteration $k$, Eqs. 4.5a and 4.5b are used to determine (1) how long the unit will remain in the up state and (2) what state the unit will transition to. If $TTF_k$ is less than $TTD_k$, then the unit moves to the failure state for duration $TTR_k$. Otherwise, the unit is in the derated state for duration $DD_k$. In this way, as shown in Fig. 4.5, an operating cycle can be obtained for the unit of interest.

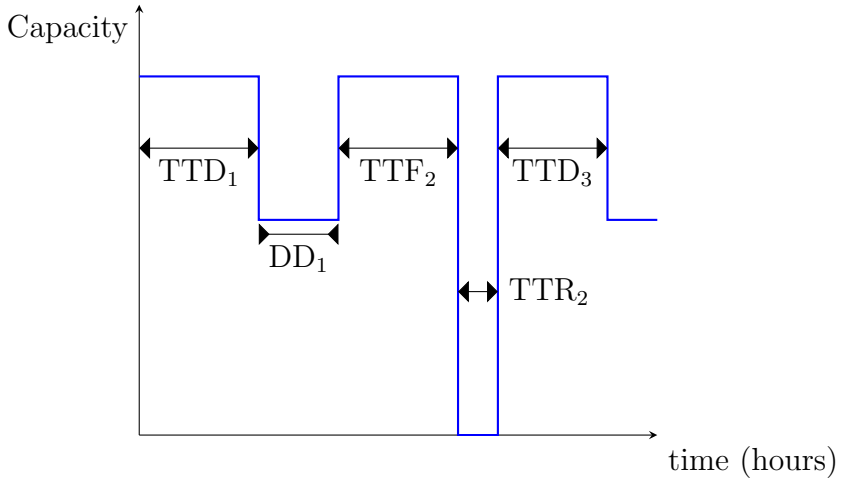


Figure 4.5: Operating cycle for a three-state unit.

### 4.3.3 Adequacy Indices

Adequacy evaluation primarily uses probabilistic methods; therefore, most adequacy indices involve expectations. Expected values provide a look at the long-term value of system parameters, a key strength over deterministic values that lack stochastic scrutiny.

Equivalent Unplanned Derated Hours

As defined by the North-American Electric Reliability Corporation (NERC), the equivalent unplanned derated hours (EUDH) converts each instance of unplanned derating $D_i$ into equivalent full outage hours [60]:

$$EUDH = \frac{\sum_{D_i} \text{(derating hours)*(MW Reduction Size)}}{\text{(Net Maximum Capacity)}} \quad \text{[hr]} \tag{4.6}$$

Loss of Load Expectation

The loss of load expectation (LOLE) is the average duration, in days or hours, that the generation capacity will be less than the daily or hourly peak load, respectively. For a simulation of $N$ sample years, with each year $i$ having $LLD_i$ days (or hours) of load loss, the LOLE is:

$$LOLE = \frac{\sum_{i=1}^{N} LLD_i}{N} \quad \text{[days/yr, hr/yr].} \tag{4.7}$$

While not indicative of the severity, frequency, or duration of each loss-of-load event, it is still a heavily used probabilistic method in generation capacity studies.

Loss of Energy Expectation

The loss of energy expectation (LOEE) index is:

$$LOEE = \frac{\sum_{i=1}^{N} ENS_i}{N} = \frac{\sum_{i=1}^{N} 8760 * DNS_i}{N} \quad \text{[MWh/yr]} \tag{4.8}$$

where $ENS_i$ and $S$ are as defined above, and $C_i$ represents the loss of load for state $i$. The LOEE, through $C_i$, incorporates the severity of the loss-of-load generation deficiencies in an attempt to be more informative than the LOLE. When alternative energy sources are being considered, it may be more useful to examine this metric over the LOLE [59].

## 4.4 Drought Modeling

As previously highlighted, a significant portion of the electricity generation uses once-through and recirculating cooling technologies that require large amounts of cooling water. In periods of drought, the energy sector faces competition for water use with sectors such as agriculture. Additional constraints come in the form of river and reservoir temperature and environmental protections put in place by federal regulations [38].

Since once-through cooling returns the water to the river it was drawn from, as the stream passes each once-through plant, the temperature of the cooling water rises. In some cases, this water may not fully dissipate this additional heat before reaching the next plant's cooling intake. If there is a heat wave, the temperature of the water may be high even before any plant has withdrawn water. As a result, generation capacity may depend on the water conditions upstream.

To address the derating implications of reduced water availability, the stream-plant model developed in [61] is used. Their model characterizes the CWA's effluent and temperature requirements, converting them into power plant operating points for system analysis.

### 4.4.1 Thermal Variance

For once-through cooling systems, the temperature at the edge of the mixing zone, $T_{edge}$ in Fig. 4.6, can be measured directly. More often than not, however, compliance is confirmed using an equation of the form:

$$T_{edge} = \frac{(kq_{us}T_{us}) + q_{pp}T_{pp}}{kq_{us} + q_{pp}} \leq T_{edge}^{max} \tag{4.9}$$

where
$q_{us}$ is streamflow upstream from the plant [vol/time],
$T_{us}$ is temperature upstream from the plant [°C],
$q_{pp}$ is power plant effluent flow [vol/time],
$T_{pp}$ is power plant effluent temperature [°C], and
$k$ is a regulation-defined plant discharge fraction.
$T_{edge}^{max}$, the maximum temperature allowed at the edge of the mixing zone, varies with the time of year.

Previous work used this model to determine the minimal thermal variance

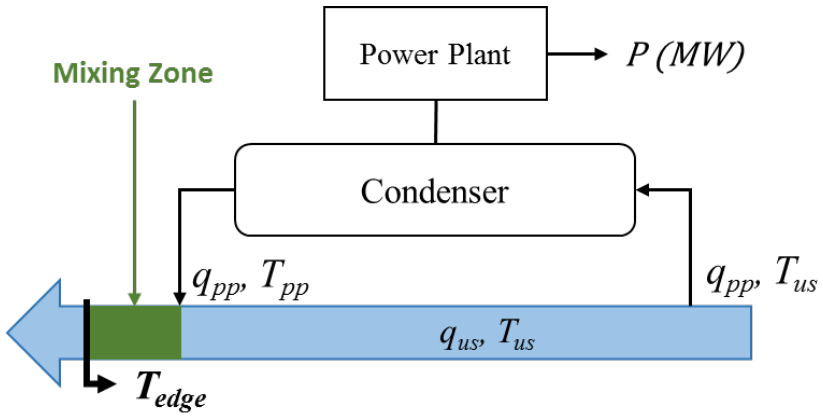


Figure 4.6: Mixing zone temperature and streamflow measurements.

that a set of generators can request to maintain operating points [61], where

$$TV = T_{edge} - T_{edge}^{max} \tag{4.10}$$

For this work, the drought scenarios will be extended to analyze the possibility of temperature and/or streamflow-driven curtailments.

### 4.4.2 Modeling Water Constraints

A heat balance model is used to relate the power output $P$ to the power plant effluent flow rate and temperature [62, 63]:

$$P = \frac{3.6\rho c_p q_{pp}(T_{pp} - T_{us})}{(HR - 3600 - \beta)} \tag{4.11}$$

where $T_{pp}$, $q_{pp}$, $T_{us}$ and $q_{us}$ are as defined previously and shown in Fig. 4.6. Constants $\rho$ and $c_p$ are the density and specific heat capacity of water respectively; these values are assumed to remain constant over the range of power plant outputs. $HR$ is the power plant heat rate, and $\beta$ is the amount of heat that leaves the power plant as flue gas. The HR and beta for different plant configurations, obtained from the EIA, are shown in Table 4.1 [64].

The maximum power output under different flow and temperature conditions was then determined by maximizing Eq. 4.11 subject to:

Table 4.1: Generator Heat Rate and Heat Loss Factors

| **Fuel Type** | **Prime Mover** | **Heat Rate** | $\beta$ |
|---|---|---|---|
| Coal | Steam Turbine | 10142 | 1217 |
| Nuclear | Steam Turbine | 10452 | 0 |
| NGas | Steam Turbine | 10416 | 1218 |
| NGas | Gas Turbine | 11590 | 3477 |
| NGas | Internal Combustion | 9917 | 2479 |
| NGas | Combined Cycle | 7619 | 1524 |

- Constraints on the temperature at the edge of the mixing zone:

$$T_{edge} \leq T_{edge}^{max} = 32°\text{C} \tag{4.12a}$$

$$T_{edge} \leq T_{us} + 2.8°\text{C} \tag{4.12b}$$

  The temperature at the edge of the mixing zone is approximated using Eq. 4.9 with $k = 0.25$, a value that is commonly used in power plant permits in Illinois [65, 66, 67, 68].

- Constraints on the effluent flow rate due to pump capacity (Eq. 4.13a) and the fact (Eq. 4.13b) that the power plant cannot exceed water body streamflow:

$$q_{pp} \leq 40 \text{ m}^3/\text{s} \tag{4.13a}$$

$$q_{pp} \leq q_{us} \tag{4.13b}$$

- Constraints on the temperature of the effluent:

$$T_{pp} - T_{us} \leq 10°\text{C}$$

  If the temperature of the effluent is too high, it will raise the condensing temperature of the steam cycle and therefore reduce the power output and efficiency of the power plant. 10°C is a typically quoted $\Delta T$ for the power plant condenser model [69].

## 4.5 Example Derating Calculation

With the optimization problem defined in Section 4.4, the capacity of the generator outlined in Table 4.2 can be directly related to the streamflow and stream temperature in order to create $\delta$. Sampling the distributions will allow for a probabilistic look at the derating probability and amount (in MW).

Table 4.2: Generator Parameters

| **Unit Fuel** | Coal |
|---|---|
| **Prime Mover** | Steam Turbine |
| **Max MW** | 1144 |
| **Heat Rate** | 10142 |
| $\beta$ | 1217 |

Daily average summer streamflow and air temperature data were taken from a representative power plant site along the Illinois River from 1990 to 2016. Air temperature data were used as a surrogate for water temperature since there is a longer historical record for air temperature; stream temperature data in Illinois generally only go back to 2012. Over long periods of time, air temperature is the primary determinant of stream temperature [70].

### 4.5.1 State Sampling Method

Empirical probability distributions of these data can be seen in Fig. 4.7. As shown, the streamflow distribution is approximately log-normal and the temperature distribution is approximately normal.

A total of 250 samples were taken from both the upstream temperature and flow distributions and combined to form 62,500 data points, representing a range of possible weather conditions. The optimization problem was solved for each combination of flow and temperature in order to determine the magnitude of derating.

Figure 4.8 shows a ten-bin histogram of the generator capacity, the results of which appear feasible. While there are instances of derating, they are not so common that the generator becomes cost-inefficient to operate.

Converting these results into an expected derating amount and probability is done by calculating $\delta = P[X < x]$, the probability that the unit will

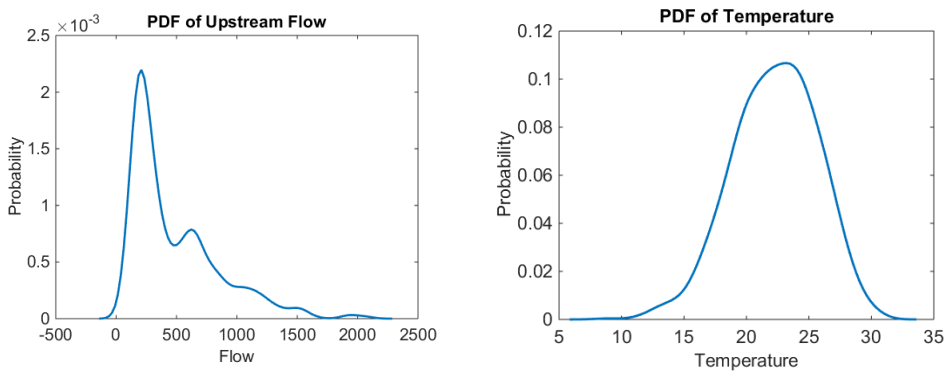


(a) Upstream flow distribution.

(b) Temperature distribution.

Figure 4.7: Probability distributions of the temperature and streamflow.

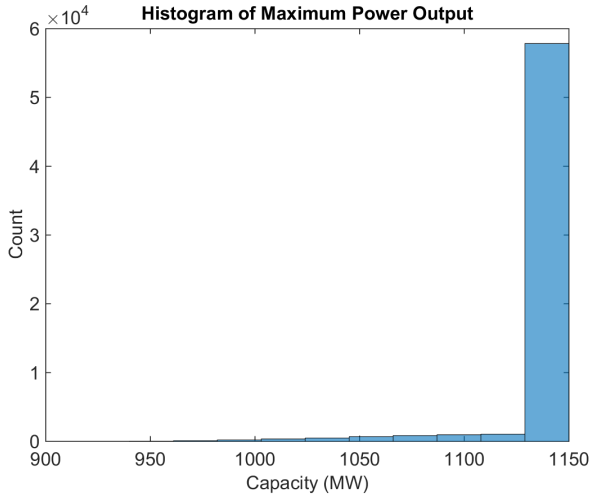


Figure 4.8: Histogram of the generation capacity available.

only have capacity $x$ (in MW) available. Table 4.3 shows the probabilities associated with different derating percentages, denoted $G_{\%}$. Using the results in Table 4.3 to create the derating probability $\delta$, the state sampling method can be applied to a three-state (on, off, derated) generating model.

For the initial results, a sample size of 250 was arbitrarily chosen; however, a smaller number may give accurate results while also reducing computation time. Table 4.4 shows the resulting $\delta$-values as the number of temperature and streamflow samples was varied from 50 to 500. For each of these sample sizes, multiple simulations were run to obtain an average probability. As the number of samples decreases, there is more significant variation when determining $\delta$ at 95% derating; however, the difference decreases with the derating percentage.

Table 4.3: Unit Capacity Probabilities

| $x$ | $P[X < x]$ |
|---|---|
| 1087 MW ($G_{95\%}$) | 0.0426 |
| 1030 MW ($G_{90\%}$) | 0.0125 |
| 973.1 MW ($G_{85\%}$) | 0.0084 |
| 915.8 MW ($G_{80\%}$) | 0 |

Table 4.4: The Effect of Sample Size on Derating Probabilities

| | $P[X < x]$ for Different Sample Sizes | | | |
|---|---|---|---|---|
| $x$ | 50 | 100 | 250 | 500 |
| $G_{95\%}$ | 0.0528 | 0.0405 | 0.0426 | 0.0403 |
| $G_{90\%}$ | 0.0140 | 0.0119 | 0.0125 | 0.0126 |
| $G_{85\%}$ | 0.0013 | 0.0013 | 0.0008 | 0.0014 |
| $G_{80\%}$ | 0 | 0 | 0 | 0 |

Two-Unit Example

A two-unit example is used to show the significance of the derating parameter; the results are summarized in Table 4.5. Two 900 MW units with forced unavailabilities $\lambda_1 = 0.08$, $\lambda_2 = 0.04$ and derating probabilities $\delta(G_{85\%}) = 0.0013$ are used to meet demand $D$. The first demand represents a scenario in which at least one unit must be available at rated capacity, the second requires both generators available.

Table 4.5: Reliability Indices

| | | EDNS | LOEE | LOLE |
|---|---|---|---|---|
| $D = 900$ | without $\delta$ | 2.646 | 23178 | 25.75 |
| | with $\delta$ | 3.150 | 27594 | 30.66 |
| $D = 1200$ | without $\delta$ | 37.63 | 329603 | 1018 |
| | with $\delta$ | 38.91 | 340872 | 1042 |

In examining the annualized indices, even when the probability of derating is a fraction of a percent, there is a noticeable increase in the LOEE and LOLE.

### 4.5.2 State Duration Sampling Method

In the state sampling method, the system states were sampled from a predefined distribution. However, past water availability can play a role in present generation capacity. Therefore, the state duration sampling method will be used, the results of which will be compared to the state sampling method. To obtain the event durations (i.e., MTTD and MDD), the model in Section 4.4 is used on chronological ($temperature$, $streamflow$) data pairs.

Using sequential data allows for a seasonal breakdown of the results; seasonal divisions are created using the meteorological distribution given in Table 4.6. Figure 4.9 shows how the temperature trends and peaks for the state of Illinois are conducive to meteorological divisions [71].

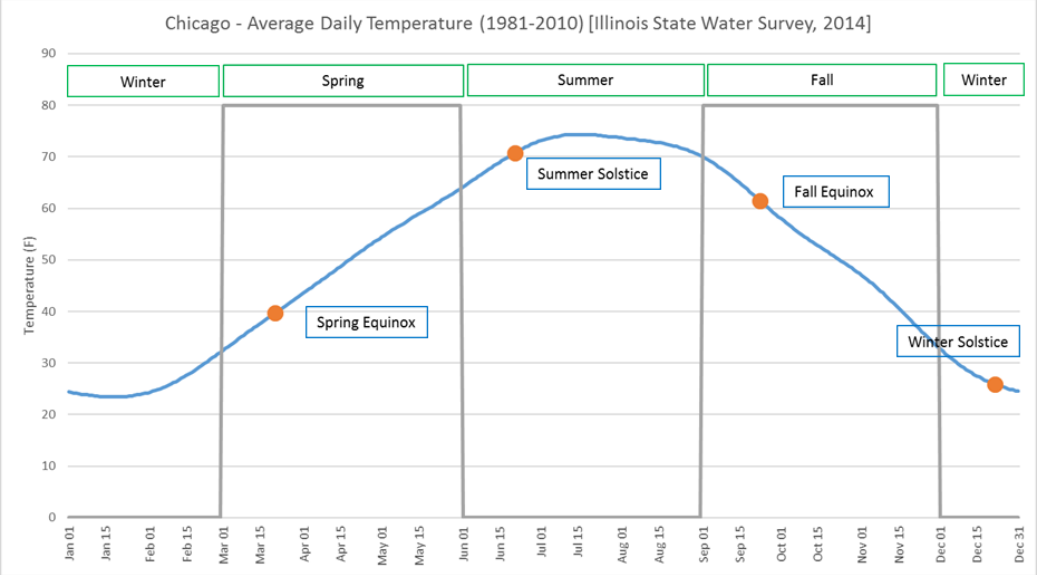


Figure 4.9: Comparison of seasonal divisions using meteorological (lines) and astronomical (orange dots) divisions.

Table 4.6: Start and End Dates of Each Season

| Season | Start Date | End Date | Days | Hours |
|---|---|---|---|---|
| Spring | 3/1 | 5/31 | 92 | 2208 |
| Summer | 6/1 | 8/31 | 92 | 2208 |
| Fall | 9/1 | 11/30 | 91 | 2184 |
| Winter | 12/1 | 2/28 (2/29) | 90 (91) | 2160 (2184) |

Summer, being the hottest season, should have derating instances that are more frequent, last longer, and have a larger reduction in MW capacity. Table 4.7 lists the median of the mean ($\mu$) and standard deviation ($\sigma$) of the summer capacity between 1991 and 2016. Since the mean is fairly close to the rated capacity and the standard deviation is orders of magnitude smaller, the derating potential of other seasons is negligible. Therefore, only the summer Illinois plant data was used for the following simulation.

Table 4.7: Median Plant Statistics by Season for a 1145 MW Coal Unit

| Spring | | Summer | | Fall | | Winter | |
|---|---|---|---|---|---|---|---|
| $\mu$ | $\sigma$ | $\mu$ | $\sigma$ | $\mu$ | $\sigma$ | $\mu$ | $\sigma$ |
| 1144.25 | 1.29E-10 | 1138.41 | 20.62 | 1143.88 | 2.51 | 1144.25 | 1.68E-11 |

Table 4.8 shows the $G_{90\%}$, MTTD, and MDD for summers in which the probability of derating was non-zero. Note that the years with the lowest (MTTD, MDD) pairs are 2005 and 2012, years that the Illinois Governor and Illinois State Water Survey have acknowledged as significant drought years [72, 73]. Additionally, many of the Illinois curtailments cited in NREL's curtailment report and shown in Table 2.1 were once-through coal plants.

Table 4.8: Coal-Steam Statistics for an 1118 MW Unit

| Year | $\mu$ (MW) | $\sigma$ (MW) | $G_{90\%}$ | MTTD (days) | MDD (days) |
|---|---|---|---|---|---|
| 1991 | 1099.3 | 40.5 | 6.52 | 21.5 | 2.0 |
| 1995 | 1104.6 | 38.9 | 3.26 | 44.5 | 3.0 |
| 1997 | 1110.4 | 24.7 | 1.09 | 45.5 | 1.0 |
| 1999 | 1107.1 | 35.2 | 5.43 | 21.8 | 1.67 |
| 2002 | 1110.6 | 23.5 | 1.09 | 45.5 | 1.0 |
| 2003 | 110.2 | 32.2 | 3.26 | 29.7 | 1.5 |
| 2005 | 1065.9 | 64.3 | 22.8 | 10.1 | 3.5 |
| 2006 | 1107.9 | 34.4 | 3.26 | 44.5 | 3.0 |
| 2007 | 1111.5 | 20.3 | 1.09 | 45.5 | 1.0 |
| 2011 | 1108.1 | 33.4 | 3.26 | 44.5 | 3.0 |
| 2012 | 1073.1 | 61.7 | 17.4 | 8.4 | 2.0 |
| 2013 | 1111.7 | 20.0 | 1.09 | 45.5 | 1.0 |

The other power plant type to experience severe deratings is, as can be as-

sumed from the NREL event data, the once-through nuclear plants. Example deratings are shown in Table 4.9.

Table 4.9: Nuclear-Steam Statistics for an 870 MW Unit

| Year | $\mu$ (MW) | $\sigma$ (MW) | $G_{90\%}$ | MTTD (days) | MDD (days) |
|---|---|---|---|---|---|
| 2005 | 828.36 | 49.95 | 22 | 10.14 | 3.5 |
| 2008 | 868.37 | 1.19E-13 | 3.26 | 92 | NaN |
| 2012 | 833.94 | 47.96 | 17 | 8.44 | 3.0 |

Table 4.10 shows the derating probabilities for the relevant units in the year 2005. Gas and combustion turbines use no steam, and therefore had no weather-related derating instances in this example.

Table 4.10: Summer 2005 Statistics for Different Plant Configurations

| Fuel Type | Prime Mover | $G_{90\%}$ | MTTD (days) | MDD (days) |
|---|---|---|---|---|
| Coal | Steam | 22.8 | 10.1 | 3.5 |
| Nuclear | Steam | 22 | 10.6 | 3.5 |
| NGas | Steam | 7 | 17 | 1.75 |
| NGas | CC | 5 | 29 | 2.5 |

To determine the effects of summer deratings on system reliability, the state sampling method was applied using the MTTD and MDD for 2005. Given that these parameters came from an assessment of summer temperature and streamflow data, TTD and DD are only applied during the summer hours. An increasing number of Monte Carlo simulations are run, with the EUDH being calculated at the end of each summer. To increase the resolution of the simulated years, the MTTD and MDD are converted into hourly times. The MTTF and MTTR are obtained from NERC's Generating Availability Data System (GADS), which provides aggregated reliability data organized by power plant fuel type and prime mover; specific values are provided in Table A [74].

The 2005 EUDH as a function of the number of simulations is shown in Fig. 4.10. After approximately 100,000 simulations, the EUDH converges to 132.64 summer hours in 2005 and 99.62 summer hours in 2012.

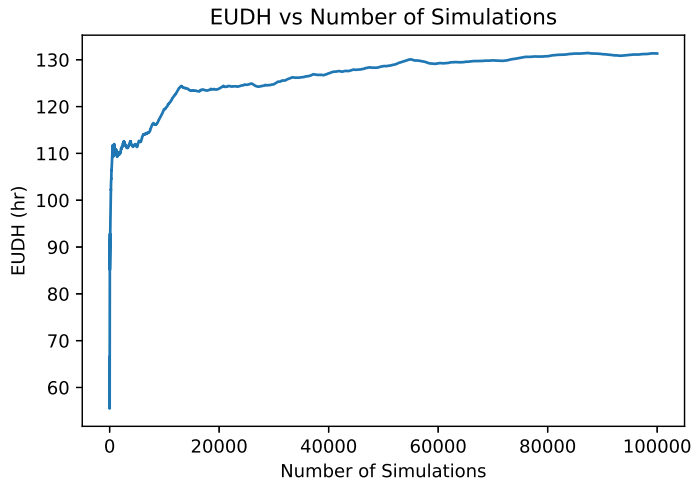


Figure 4.10: 2005 EUDH vs. the number of experiments.

## 4.6 Conclusion

This chapter introduced cooling-water based derating parameters into Monte Carlo reliability analysis. For the state sampling method, the derating was the result of taking temperature and streamflow samples from a derived distribution. For the state duration sampling method, chronological (temperature, streamflow) pairs were used to calculate each duration's duration, as well as the time between derating events.

Based on the calculations done throughout the entire year, the only season that showed significant derating instances was summer. This was expected, given the intake and discharge temperatures were the most common reason why generators with cooling-water limitations were forced to reduce their capacity. In order to determine the significance of limited water on system resiliency, standard reliability metrics, such as the equivalent unplanned derated hours (EUDH) and the loss of load expectation (LOLE), were used.

Multiple generators derating to 90%, even if not substantial for one unit, will be a problem in the context of weather deratings. Weather-based derating affects multiple units simultaneously, and is the result of external factors outside of human control. Therefore, maintaining reliability requires knowing beforehand which units will experience weather-driven deratings via methods such as those proposed in this chapter.

# CHAPTER 5

# GENERATION ASSET VALUATION

## 5.1 Overview

Although California water use originally followed a prior appropriation doctrine, in which water allocation is made on a "first-come, first-served" basis independent of land ownership, they moved to a mixed riparian-appropriation doctrine. Under this hybrid doctrine, in certain cases, appropriation users must yield their water to riparian landowners whose water use is deemed superior [75].

Given the GAO's projected water shortages by 2023, it is likely that heavy water users such as once-through coal and nuclear plants will see additional instances of derating or shutdown. This potential for reduced generation capacity affects the bidding strategies and profits of generation companies (GenCos) that own derated units.

While the previous chapter looked at assessing potential changes in revenue and market power with cooling water costs, this chapter focuses on another aspect of deregulated electricity markets. In particular, this chapter uses the water cost parameter in order to determine to what extent cooling water availability can affect GenCo profits.

## 5.2 Price-Based Unit Commitment

Traditionally, unit commitment (UC) has been driven by minimizing generation costs while still meeting system demand. In the deregulated market, however, GenCos are now able to focus on the maximization of their profits

irrespective of load requirements. If $C_i(P)$ represents the cost of power $P$ generated by generator $i$, as in Eq. 5.1:

$$C_i(P) = a_i + b_i P + c_i P^2 \tag{5.1}$$

then this profit maximization can be achieved by maximizing the difference between the revenue and operating costs:

$$F = max \sum_k \left[\rho_t P_k - C_k(P_k)\right] \tag{5.2}$$

where $P_k$ is MW generation of plant $k$ and $\rho$ is the market clearing price. The maximization can become a minimization by negating each term in the summation. For determining a unit commitment schedule in the day-ahead market, this optimization will be calculated for each hour $t = 1, 2, \ldots, 24$:

$$\begin{aligned} F &= min \sum_k \sum_t \left[C_k(P(k,t)) - \rho_t P(k,t)\right] I(k,t) \\ &= min \sum_k \sum_t \left[a_k + (b_k - \rho(t))P(k,t) + c_k P(k,t)^2\right] I(k,t) \\ &= min \sum_k \sum_t L(i,t) I(k,t) \\ & \qquad P_{min}(t) \leq P(k,t) I(k,t) \leq P_{max}(t) \end{aligned} \tag{5.3}$$

This unit commitment is referred to as the price-based (or profit-based) unit commitment (PBUC) because an accurate profit assessment relies heavily on $\rho$, the forecasted market price.

Since GenCos and TransCos are now separate entities, congestion information is not available to the GenCo. However, congestion is captured in the locational marginal price, so as long as the GenCo has accurate forecasting tools at its disposal, the congestion will have already been incorporated.

The profit maximization for each period depends on whether the generator is on or off ($I(k,t) = 0$ or 1), so dynamic programming will be used to determine the optimal on-off scheduling for each generator for each hour as shown in Fig. 5.1.

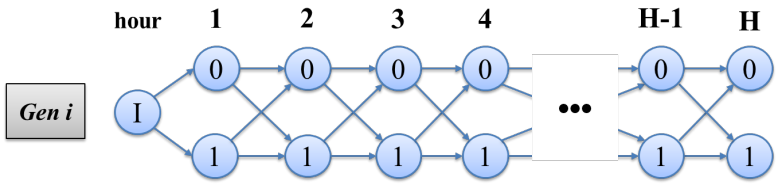


Figure 5.1: The individual stages of the dynamic program.

### 5.2.1 Computational Considerations

In an attempt to avoid the over or under-committing of generation capacity based on PBUC results, the multi-generator PBUC methodology in [76] is used. Outlined in the flowchart of Fig. 5.2, for each period $t$, the total capacity of the current commitment schedule is compared to the period's demand. If the capacity is too high, the price signal $\rho_t$ will be decreased in an attempt to get some generators to decommit; the opposite will happen if not enough generation is committed. Every few iterations, $\Delta\rho$ is reduced in order to approach a fine-tuned commitment schedule.

With respect to the computational burden, enumeration indicates a PBUC problem spanning $H$ periods has $2^H$ state combinations for a single generator. In the case of the IL200, a day-ahead bidding schedule requires $G_i 2^{24}$ calculations, where $G_i$ is the number of generators belonging to GenCo $i$. If the joint-PBUC is being applied, where each generator adjusts its schedule for $q$ iterations, the number of loops increases to $qG_i * 2^{24}$.

Reducing the number of calculations required can be done by observing the *principle of optimality*, which states that an optimal path must contain only optimal subpaths. As shown in Fig. 5.3, if a number of sub-periods $T$ is specified such that $T = 24/N$, where $N$ is the length of each sub-period, then the number of calculations reduces to $qNG_i * 2^{24/m}$.

If the PBUC formulation of Eq. 5.3 is used, commercial power systems software can be used to solve the profit maximization by setting the $b_i$ cost-coefficient to $(b_i - \rho_t)$. Additional functionality of PowerWorld Simulator, the software used to assist in this analysis, is discussed in Appendix C.3.5.

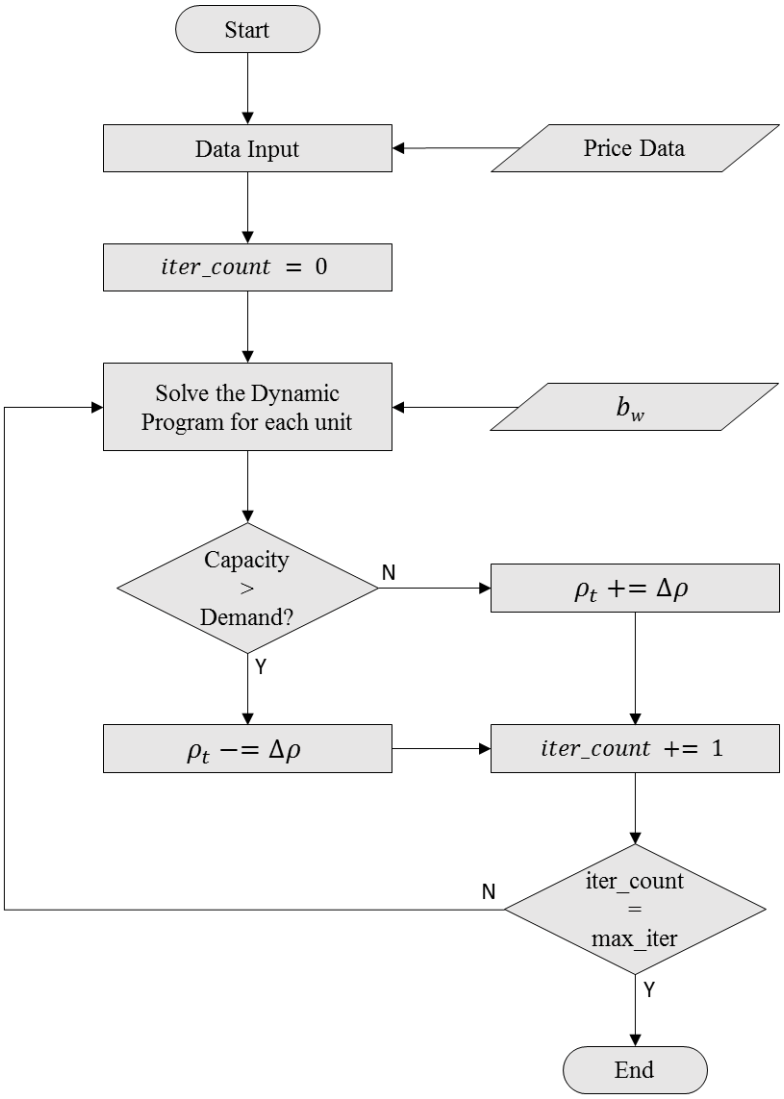


Figure 5.2: Flowchart outlining the joint-PBUC formulation for each period.

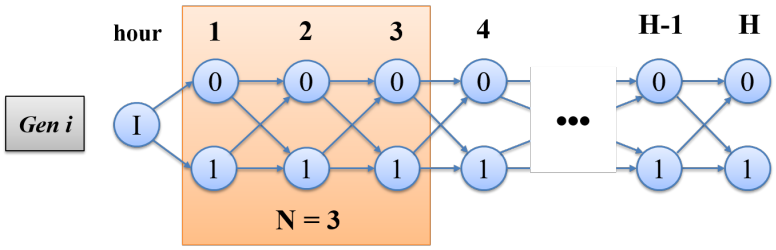


Figure 5.3: Using a sub-period to reduce the number of calculations required for the dynamic programming solution.

## 5.3 Value-at-Risk (V@R)

The move to a deregulated, competitive electric market comes with a new set of risks that depend on the bidding strategies adopted by GenCos. Rather

than guaranteed sales at marginal cost, the value of a generator is realized by accepted bids. Deregulation creates situations where generation bids are above the market clearing price. In such a situation, the generation unit will not provide power to the electricity market, resulting in a loss of potential profit. In the financial field, one of the metrics used to quantify this risk is the value-at-risk (V@R), a metric gaining traction in deregulated electricity market analysis.

The V@R attempts to estimate how much value an asset could lose for a given confidence level and time horizon. The confidence level is a percentage used to specify the certainty of the calculated V@R, typically set to 95%, 99%, or 99.9%. For example, if the confidence level of the V@R calculation is 95%, $100\% - 95\% = 5\%$ of the time the portfolio's losses will be less than the V@R. For the asset in Fig. 5.4, if its estimated value is \$50 million with a standard deviation of \$4.85 million, there is a 5% chance the asset will suffer a loss less than \$42 million.

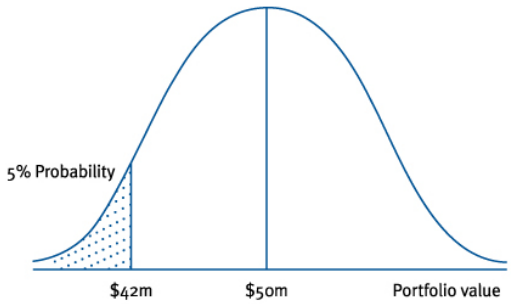


Figure 5.4: Calculation of the value-at-risk based upon the normal distribution.

### 5.3.1 V@R vs. Conditional V@R

While V@R is still a commonly used metric for assessing losses, a key downside comes from the fact that the losses beyond the tail of the distribution are not assessed. To measure this likelihood, the conditional V@R, also known as the expected shortfall, has been created to build upon the V@R. As its name implies, the CV@R measures the average of the losses that occur beyond the V@R; Fig. 5.5 visualizes this distinction by highlighting the tail red.

The smaller the CV@R the better, since it means that the losses beyond the V@R are also small.

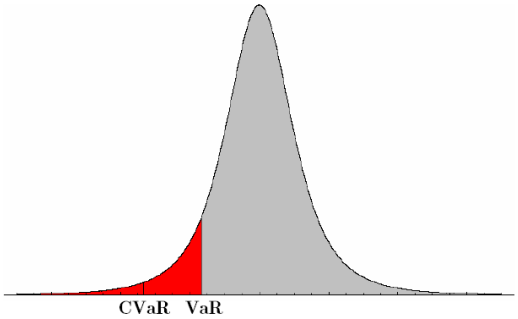


Figure 5.5: Visualization of the difference between conditional V@R and V@R.

## 5.4 Water Valuation

In order to incorporate water usage into the electricity market framework, a water cost parameter $b_w$, in \$/MWh, will be added to the fuel cost. This section outlines how existing literature has derived water costs and describes how to arrive at a "water as a fuel" cost. This water-fuel cost requires three terms: a [\$/vol] cost of water, a [vol/MWh] water usage factor for thermoelectric plants, and a profit-margin scaling parameter.

### 5.4.1 Cost of Water by Volume

One methodology used to calculate the cost of water involved analyzing the capital costs in the retro-fitting of open-loop cooling systems with closed-loop-tower technologies in the state of Illinois [41]. Water usage data and power plant capital costs were obtained from EIA and USGS water withdrawal data for Illinois. An annual cooling cost, the sum of the annualized capital and operations and maintenance costs, was calculated using:

$$C_a = \left[\frac{i(1+i)^t}{(1+i)^t - 1}\right] C_c N + C_{O\&M} G \tag{5.4}$$

where
$i$ is the annual interest rate [%],
$t$ is the cooling system's expected lifetime [yrs],
$C_c$ is the retrofit capital cost [$/MW],
$N$ is the plant's nameplate capacity [MW],
$C_{O\&M}$ is the operations and maintenance cost [$/MWh], and
$G$ is the annual generation of the power plant [MWh/yr].

An assessment of the cooling costs found an approximate water cost of 0.03-0.06 $/m$^3$. This methodology was applied in this work because (1) it used power plant data for the state of Illinois, and (2) the break-even cost was derived via comparison of power plant cooling technology costs.

### 5.4.2 "Break-Even" Water Cost

Other than retro-fitting cooling technologies, analysis of a "break-even" cost of water can be used to derive a water-fuel cost. The total cost of wet cooling and the total lifetime cost of dry cooling intersect at this break-even cost, which engineers then use to evaluate power plant cooling systems.

Derived from an Electric Power Research Institute (EPRI) report, the cost of producing "usable" water is broken down into acquisition, delivery, and treatment [77]. The total cost represents the break-even cost of water, the specific values of which are shown in Table 5.1.

Table 5.1: U.S. Water Costs [$/1000 gal]

| | Minimum | Low | Median | High |
|---|---|---|---|---|
| Acquisition | <$0.01 | $0.05 | $0.15 | $0.50 |
| Delivery | <$0.01 | $0.13 | $0.57 | $1.20 |
| Treatment | $0.10 | $0.25 | $1.00 | $4.00 |
| Total | ∼$0.10 | $0.43 | $1.72 | $5.70 |

### 5.4.3 Power Plant Water Usage

In order to convert the [$/volume] cost derived into a [$/MWh] fuel cost, a [vol/MWh] conversion factor is required. This parameter can be obtained

from EIA-923 and the NREL report on water usage factors, with gaps in one data source filled using approximations from the other.

While the NREL data is the result of a literature review that includes more than just the EIA data, additional EIA cooling data provided after the report's publication can be added on. However, the data provided by EIA needs to be aggregated in order to obtain the desired power plant water usage factors.

In particular, EIA-923 Schedule 8D provides the monthly water consumption and withdrawal estimates for power plants grouped by cooling technology. These monthly values are aggregated into annual consumption and withdrawal volumes. In order to determine the amount of water used per MWh, the volume is divided by the year-to-date net generation, provided by EIA-923 Schedule 1.

### 5.4.4 Profit Margin Scaling

There is one additional step before adding this water cost to the market analysis, based upon an assumption about the water treatment and delivery. In existing regulations, many of the water costs are internalized, and there are operation and maintenance costs for this water regardless of the end-user. Therefore, instead of using the direct cost of water, the average 10% profit margin of U.S. water utilities will be considered the "external cost" [78, 79].

For example, if the effective cost of water for an open-loop coal plant with a steam turbine comes out to be 1.50 \$/MWh, then the "total fuel cost", which is added to the linear coefficient of the quadratic equation, comes out to be

$$\bar{b} = b_i + b_w = b_i + (0.10)1.50 = b_i + 0.15 \ \ \$/\text{MWh}$$

The 0.15 \$/MWh is the external cost of water viewed-by and charged-to the generation producers.

## 5.5 PJM Example

The process outlined in Fig. 5.6 is demonstrated from the perspective of the PJM Interconnection, a regional transmission organization (RTO) whose

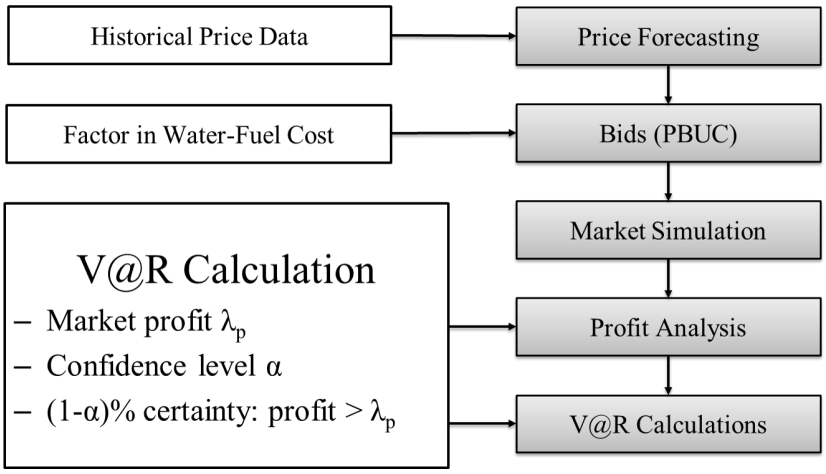


Figure 5.6: PBUC process for an individual GenCo.

coverage area is shown in Fig. 5.7 [80]. Note that the PJM territory is all owned by electric utility Commonwealth Edison (ComEd). ComEd price and load data for the day-ahead and real-time markets are publicly available on PJM's website, and are used for this analysis [81].

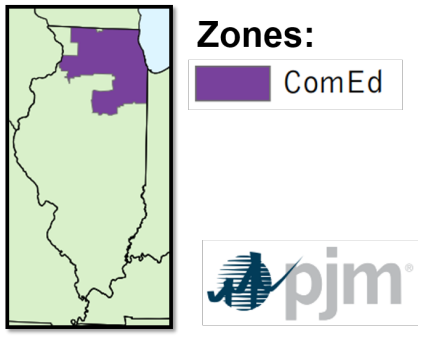


Figure 5.7: PJM Interconnection's territory within the state of Illinois, all of which belongs to electric utility Commonwealth Edison (ComEd).

The first step is to develop an hourly bidding schedule using the day-ahead price and load forecast data. The joint-PBUC, with water cost $b_w$ factored in, is run for every generator in order to generate a unit commitment schedule. The resulting schedule for PJM with and without the water costs ("initial" and "final", respectively) is listed in Table 5.2. Note that some units turned off after the demand check, indicating an initial over-commitment of generation.

Table 5.2: IL-200's PJM Region: Unit Commitment Schedule

| Unit | PBUC with Water Cost | PBUC without Water Costs |
|---|---|---|
| 1 | 10110000001101111111110 | 10110001001101111111110 |
| 2 | 11111111111111111111111 | 11111111111111111111111 |
| 3 | 11111111111111111111111 | 11111111111111111111111 |
| 4 | 11111111111111111111111 | 11111111111111111111111 |
| 5 | 00000000000000000000000 | 00000000000000000000000 |
| 6 | 00000000000000000000000 | 00000000000000000000000 |
| 7 | 00000000000000000000000 | 00000000000000000000000 |
| 8 | 00000000000000011000000 | 00000000000000011100000 |
| 9 | 00000000000000011000000 | 00000000000000011000000 |
| 10 | 11111111111111111111111 | 11111111111111111111111 |
| 11 | 00000000000000000000000 | 00000000000000000000000 |
| 12 | 00000000000000000000000 | 00000000000000000000000 |
| 13 | 11111111111111111111111 | 11111111111111111111111 |
| 14 | 11111111111111111111111 | 11111111111111111111111 |
| 15 | 11111111111111111111111 | 11111111111111111111111 |
| 16 | 11111111111111111111111 | 11111111111111111111111 |
| 17 | 11111111111111111111111 | 11111111111111111111111 |
| 18 | 11111111111111111111111 | 11111111111111111111111 |
| 19 | 11111111111111111111111 | 11111111111111111111111 |
| 20 | 11111111111111111111111 | 11111111111111111111111 |
| 21 | 00000000000000000000000 | 00000000000000000000000 |
| 22 | 11111111111111111111111 | 11111111111111111111111 |
| 23 | 11111111111111111111111 | 11111111111111111111111 |
| 24 | 11111111111111111111111 | 11111111111111111111111 |
| 25 | 00000000000000111111100 | 00000000000000111111100 |
| 26 | 00000000000000000000000 | 00000000000000000000000 |
| 27 | 00000000000000000000000 | 00000000000000000000000 |
| 28 | 11111111111111111111111 | 11111111111111111111111 |
| 29 | 11111111111111111111111 | 11111111111111111111111 |
| 30 | 11111111111111111111111 | 11111111111111111111111 |
| 31 | 11111111111111111111111 | 11111111111111111111111 |
| 32 | 11111111111111111111111 | 11111111111111111111111 |
| 33 | 10110001001101111111110 | 10110001001111111111110 |
| 34 | 11111111111111111111111 | 11111111111111111111111 |
| 35 | 11111111111111111111111 | 11111111111111111111111 |
| 36 | 11111101111111111111111 | 11111101111111111111111 |
| 37 | 00000000000000111111100 | 00000000000000111111100 |
| 38 | 00000000000000000000000 | 00000000000000000000000 |
| 39 | 00000000000000000000000 | 00000000000000000000000 |
| 40 | 00000000000000000000000 | 00000000000000000000000 |
| 41 | 00000000000011111111100 | 00000000000011111111100 |

Having run the joint-PBUC, the IL200 system is run for two days at hourly resolution. The commitment schedule developed is used for GenCo1, and the resulting profits for four generators are shown in Fig. 5.8. As expected, the introduction of additional cost $b_w$ has notably reduced the profits for some of the generators; however, hydropower, which does not use cooling water, experiences no changes.

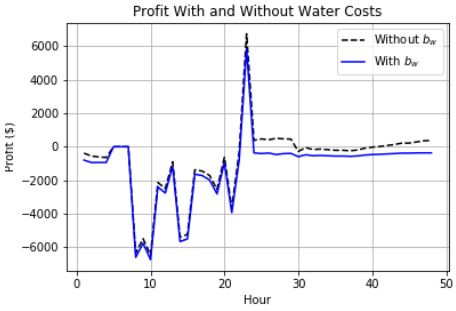


(a) Generator 1 (Nuclear, Steam)

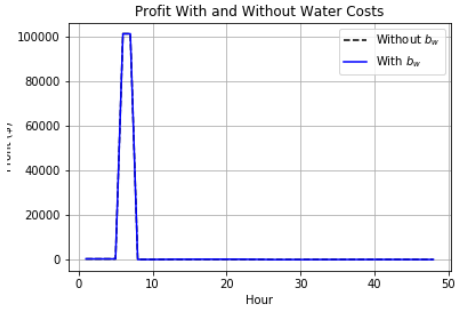


(b) Generator 2 (Hydro, NA)

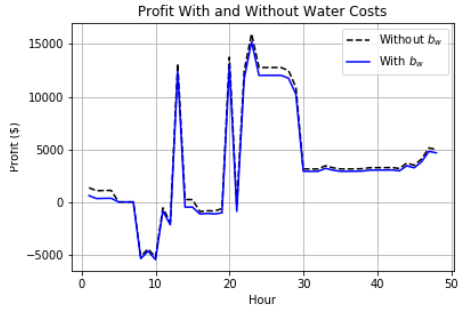


(c) Generator 3 (Nuclear, Steam)

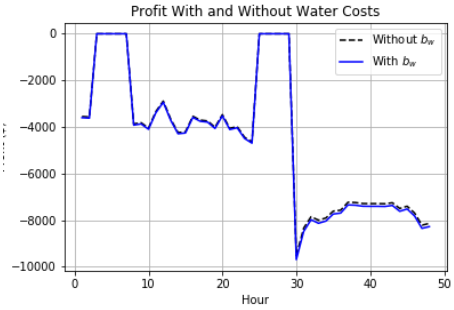


(d) Generator 4 (Coal, Steam)

Figure 5.8: Profits for representative generators with (blue) and without the water-fuel cost $b_w$.

In order to calculate the V@R and CV@R, the historical price data for the date of interest needs to be fit to a normal distribution. As shown in Figs. 5.4 and 5.5, once the profit for a given hour has been mapped to the probability of PJM clearing the market at the given price, the profit distribution can be used to calculate the V@R and CV@R directly. Fortunately, PJM provides historical real-time LMP data, which is used to generate the probability distributions for the two days.

For the real-time PJM data, the mean and standard deviation came out to be 30.2597$/MWh and 13.66$/MWh, respectively; the resulting distribution is shown in Fig. 5.9. From there, each individual day-ahead forecasted price $\rho_t$ can be converted into a probability of receiving that LMP price by calculating $P[X = \rho_t]$, the probability that the LMP turns out to be $\rho_t$. This probability is calculated for each hourly price in order to obtain probabilities that correspond to the profit in each hour.

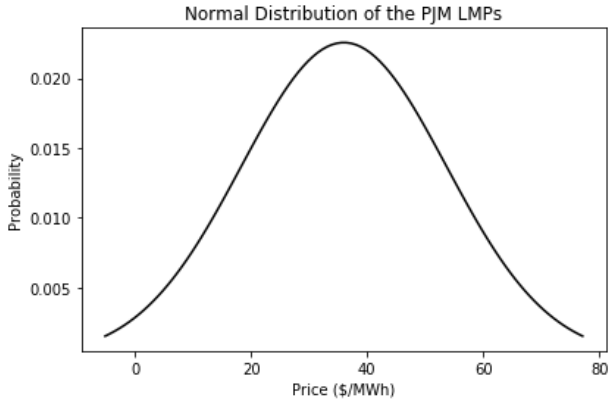


Figure 5.9: Probability distribution of the PJM LMPs.

The V@R for any generator in PJM can be calculated by specifying a confidence interval with which to measure against a unit's profit. Using a 99% confidence interval, the V@R of Generator 1 in Fig. 5.8a is $6715 without $b_w$ and $6893 with $b_w$ (denoted V@R$_w$). Factoring in the water cost has resulted in an additional $178 of potential losses for this generator with the given price forecast. The V@R and CV@R results for this generator are listed in Table 5.3

Table 5.3: Two-day V@R and CV@R Results for Generator 1

| $\alpha$ | V@R | V@R$_w$ | CV@R | CV@R$_w$ |
|---|---|---|---|---|
| 0.05 | \$6125 | \$6393 | \$5846 | \$5754 |
| 0.02 | \$6544 | \$6811 | \$6464 | \$6732 |
| 0.01 | \$6715 | \$6893 | \$6464 | \$6732 |

## 5.6 Conclusions

This section developed a water cost parameter for generation profit analysis and asset valuation. Using the price-based unit commitment over the traditional unit commitment allows GenCos to focus on the maximization of their profits without being constrained by security or demand requirements. In analyzing the profits with and without the water parameter, the dependence of generation revenue and profits can be quantified.

By adding the water cost in the PBUC formulation via the cost function, changes in unit commitment and generator profits (as well as their likelihoods) can be explicitly measured. As a result, comparing the value at risk before and after factoring in the water cost can give insight into how much of the risk associated with a GenCo's profits is tied to water availability.

# CHAPTER 6

# ELECTRIC MARKET ANALYSIS

## 6.1 Overview

From late 1996 to mid-2010, Australia was going through the Millennial Drought, their worst drought in recorded history. The severity of the drought placed higher stresses on Australian water management, particularly in the southwest at their Murray-Darling Basin [82]. In an effort to improve water efficiency and usage, Australia implemented water markets and water trading, gradually moving from long-term contracts to sales for water used.

A separate water market within the United States may not be as straightforward to implement due to the country's size, geographical differences, and state-based variations in regulation and policy. However, increasing competition for water resources has motivated California to start taking steps in that direction. The flexibility offered by a mixed policy, combined with drought stresses, encouraged California to implement a water-trading market [16]. In this market, water users specify volumes of water that they require, and water brokers facilitate the trading by identifying an appropriate seller.

In the event water markets (i.e., volume-based water sales) become more widespread in the United States, generation owners may need to start considering water acquisition as an additional cost for their power plants. Given that this volume-based sale of water is analogous to energy sales in the deregulated market, the creation of a water cost parameter for market analysis is proposed in this chapter. Applications of this water cost focus on market power assessment and potential changes in profit.

## 6.2 Deregulation

Traditionally, the electric grid was a vertically-integrated network in which a single utility was responsible for generating, transmitting, and distributing electricity in its service territory. This organizational model was managed at the state and federal levels, regulating new projects and tariff changes. However, due to:

- new generation technologies impacting economies of scale,
- growing electricity data volumes created by growth of information and communications, and
- the ability of private owners to more rapidly adopt economic and technological changes/advances,

electricity markets around the globe started restructuring during the 1990s [83]. Economists have argued that moving to a deregulated market would drive down tariffs and costs by way of competition.

In order to address economic efficiency and system reliability while limiting each firm's market power (i.e., their ability to generate additional profit through market price manipulation), the U.S. electricity industry has moved to a horizontally-integrated environment. This deregulated model unbundles the generation, transmission, and distribution systems into generation companies (GenCos), transmission companies (TransCos), and distribution companies (DistCos), each of which own and operate their respective electric grid components [17]. Additionally, load-serving entities (LSEs) aggregate user demand in an attempt to buy larger bundles of electricity at a reduced per-MWh cost.

## 6.3 Market Time Scales

In a deregulated market, the independent system operator (ISO) oversees the buying and selling of power in the Power Exchange (PX). In general, PX market participants include buyers, parties interested in buying power, and sellers (GenCos) who are supplying power. The ISO "clears" the market (i.e., sets the price of electricity) by aggregating supply and demand. From

these aggregated curves, the market clearing price (MCP), their point of intersection, becomes the system electricity price. A simplistic view of this process is shown in Fig. 6.1, with $S$ and $D$ representing the aggregate supply and demand curves, respectively.

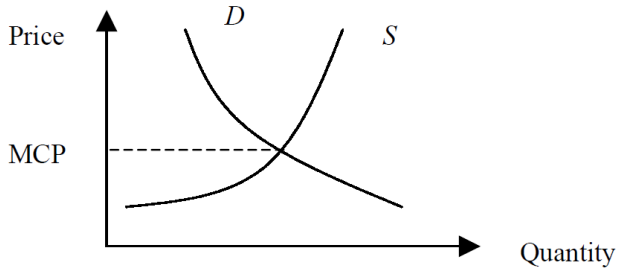


Figure 6.1: Simplistic view of the MCP [84].

### 6.3.1 Day-Ahead Market

Figure 6.2 shows the ISO's daily schedule in clearing the market for day D. The bidding resolution for day D is in hours (hrs = 00,. . . , 23); the bid/offer-to-price processes is as follows [85]:

1. load-serving entities (LSEs) aim to profit by purchasing power in the market and selling it to retail customers. GenCos, on the other hand, aim to profit by selling power at a price above their marginal cost.

2. On the morning of day D, LSEs submit demand bids and GenCos submit supply offers to the ISO. LSE and GenCo submissions include fixed and variable offers/bids for each hour of day D.

3. From there, the ISO solves a decoupled optimal power flow (OPF) to determine the locational marginal price (LMP), the regional price at which each unit of power will sell for in the market.

4. Once calculated, the ISO posts hourly demand, supply, and cost information for viewing by the market participants.

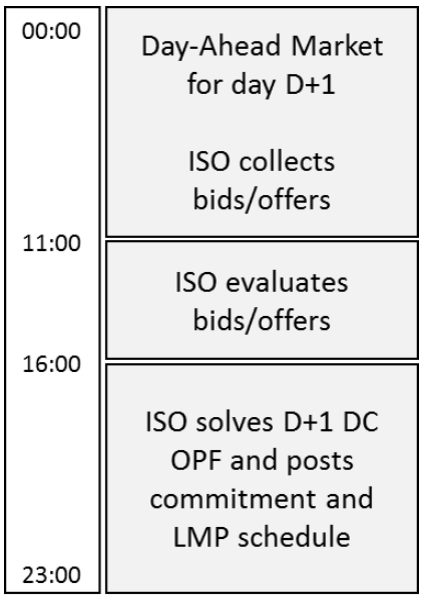


Figure 6.2: Chronological view of the ISO's day-ahead market clearing.

## 6.4 Market Power Assessment

Game theory analyzes the interaction and behavior of self-interested players within a given environment. It involves a number of players who each have a set of bidding strategies available to them; the number of strategies each player has can differ. Each outcome of the game converts the strategy set, the set of actions chosen by each player, into a payoff that quantifies their gain or loss [86].

Within this market competition players are attempting to find the Nash equilibria (NE), outcomes which stem from strategy sets where no player has incentive to change their actions. Due to players' reluctance to change their strategies, these equilibria represent stable solutions to the market being analyzed.

Within the context of deregulated markets, GenCos are competing with one another in order to sell electricity and obtain a profit. From the point of view of the ISO, however, the location and stability of the NE can indicate unhealthy competition. To address these potential problems, the ISOs do more than clear the market; they also:

- identify market collusions,
- calculate transactions and payoffs resulting from those collusions, and

- ensure limited market power for all participants

in order to facilitate clearing of the market while ensuring price stability and feasibility [87].

Buyer market power is defined as the ability of buyers to manipulate the price of electricity, using their relative generation capacity, in order to obtain additional profit. Ideally, the buyers and sellers are all small relative to the overall market size, so no player's actions can significantly affect market prices.

### 6.4.1 Herfindahl-Hirschman Index (HHI)

The Herfindahl-Hirschman index (HHI) is a well-known and accepted metric for measuring market power amongst a group of participants. It is calculated via Eq. 6.1:

$$HHI = \sum_{i=1}^{N} s_i^2 \tag{6.1}$$

where $N$ is the number of participants (i.e., GenCos) and $s_i$ is the percent market share of GenCo $i$. In the case of three GenCos with $s_1$, $s_2$, and $s_3$, the market share is

$$HHI = (25)^2 + (35)^2 + (40)^2 = 3450$$

In the case of a monopoly, one participant has 100% market share, resulting in an HHI of ($100^2 = 10000$). Therefore, the closer a market's HHI is to 10,000, the more unhealthy the competition may be.

## 6.5 Bidding Strategies

$C_i(P)$ represents the cost of power $P$ generated by generator $i$, typically represented by a quadratic polynomial:

$$C_i(P) = a_i + b_i P + c_i P^2 \tag{6.2}$$

$$= \left(\tilde{a}_i + \tilde{b}_i P + \tilde{c}_i P^2\right) * c_f \tag{6.3}$$

Equation 6.3 extracts the fuel cost $c_f$ from $a_i$, $b_i$, and $c_i$, resulting in terms $\tilde{a}_i$, $\tilde{b}_i$, $\tilde{c}_i$. In moving from generation $P_i^0$ to $P_i$, the resulting change in cost is:

$$\Delta C_i = C_i(P_i) - C_i(P_i^0) \tag{6.4}$$

$$= b_i \Delta P_i + c_i P_i \Delta P_i + c_i P_i^0 \Delta P_i \tag{6.5}$$

resulting in an incremental cost of:

$$\pi_i = \frac{\Delta C_i}{\Delta P_i} = b_i + c_i P_i + c_i P_i^0 \tag{6.6}$$

This is not the marginal cost, which is defined as the incremental cost as transaction $\Delta P_i$ approaches zero (taking the limit, mathematically):

$$\lambda_i = \frac{dC_i}{dP_i} = b_i + 2c_i P_i \tag{6.7}$$

While both curves are linear, they are not exactly the same: Fig. 6.3 depicts this difference [84].

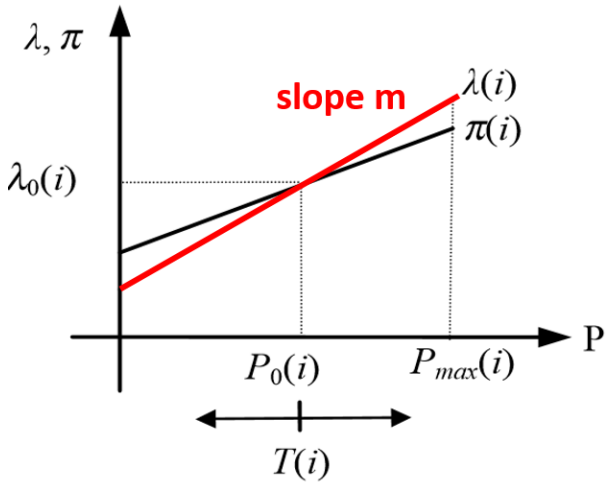


Figure 6.3: Marginal and incremental cost slopes.

If currently operating at point $P_i^0$, in order to break even with respect to operating cost, the incremental cost curve represents the highest or lowest price to accept for possible import or export $T_i$, respectively. Additionally, if the spot price is lower than the generator's marginal cost, then the utility should import power to supply its own load; its own generation will not

provide any profit.

According to economic auction theory, the hourly system cost is minimized when participants all submit bids to the ISO at marginal cost [88]. In the deregulated market, however, competition allows for flexibility in the supply bids submitted by the GenCos. The magnitude of the market deviation from the marginal cost can also indicate market manipulation.

Bids are submitted as Eq. 6.7, in particular by adjusting $m = 2c_i$, the slope of the marginal cost curve. Referring to Fig. 6.3, changing the slope of the curve rotates the red line around current operating point $P_i^0$. Since the new line is not representative of the generator's original marginal cost, it is also referred to as the bidding curve in the competitive market environment.

### 6.5.1 Creation of GenCo Marginal Cost Functions

Since each GenCo is using the market clearing price to schedule *all* of its units, a marginal cost function at the GenCo level is desirable. To derive the GenCo function, which will be a quadratic as in Eq. 5.1, individual supply and production costs will be converted into total production cost and output power $C_G(P_G)$ and $P_G$, respectively [89]. These sums are calculated by finding the operating point $P_k$ for each generator such that

$$\frac{dC_i}{dP_i} = \frac{dC_k}{dP_k} = \lambda, \quad \forall k, j = 1, \ldots, n_{Gi} \tag{6.8}$$

Obtaining each of the $[P_G, C_G(P_G)]$ data pairs used for the curve-fitting is done by adjusting $\lambda$ in increments $\Delta\lambda$, bounded by:

$$\begin{aligned} \lambda^{min} &= \min\left[\frac{dC_k}{dP_k}, \quad k = 1, \ldots, n_{Gi}\right] \\ \lambda^{max} &= \max\left[\frac{dC_k}{dP_k}, \quad k = 1, \ldots, n_{Gi}\right] \end{aligned} \tag{6.9}$$

Figure 6.4 shows this process in its entirety for a given GenCo.

### 6.5.2 Strategic Supply Function

The assessment of the GenCo's bidding behavior is done with the help of a strategic supply function, used to map its own supply to optimal bids via a

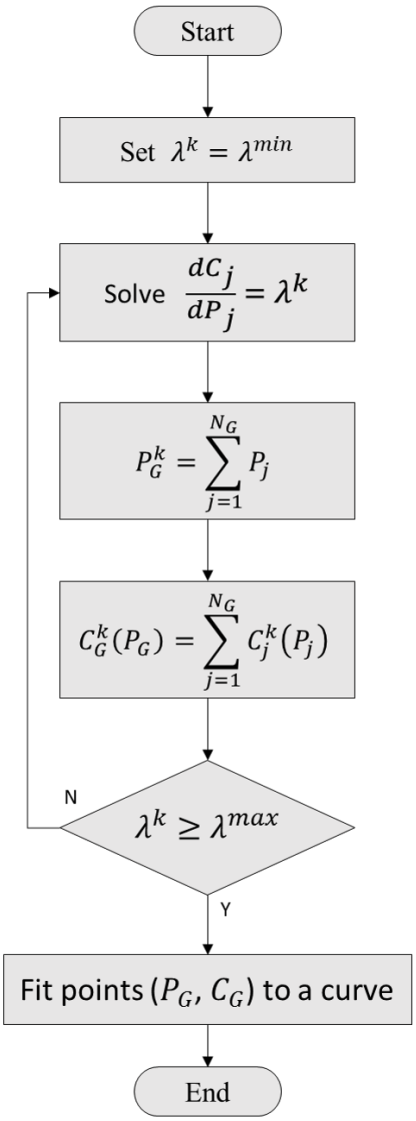


Figure 6.4: Creation of the GenCo cost function.

price signal. This section outlines the derivation the function and its use for GenCo bid assessment within the day-ahead pool-based electricity market.

Although the signal of interest for the GenCo is the price, forecasting of the cost depends not only on historical price data, but also historical load data. Before arriving at the function that maps the price to a generation bid, the relationship between the demand and price signal needs to be examined.

For a single hour within a day-ahead simulation, the demand function $D$ can be expressed as a function of the market price $\rho$:

$$D = D(\rho) \tag{6.10}$$

For $N_G$ generation companies submitting bids to this pool, the demand supplied by GenCo $i$ can be expressed as a function of the demand supplied by the other GenCos:

$$D_i(\rho) = D(\rho) - \sum_{j \neq i}^{N_G} P_j(\rho) \tag{6.11}$$

where $P_i(\rho)$ is the function that maps the spot price to GenCo $i$'s supply.

Assuming the market has cleared with spot price $\rho*$, the system demand at the system equilibrium is:

$$D(\rho*) = \sum_{i=1}^{N_G} P_i(\rho*) \tag{6.12}$$

The goal is to find out how a GenCo can calculate this equilibrium for the sake of optimizing their bidding strategy.

If the strategy GenCo $i$ adopts is optimal, then its profit, which can be expressed as

$$u_i = \rho P_i - C_{Gi}(P_i) \tag{6.13}$$

has been maximized. Differentiating with respect to the price will indicate what conditions exist around the optimum:

$$\begin{aligned} \frac{\partial u_i}{\partial \rho} &= P_i + \rho \frac{dP_i}{d\rho} - \frac{dC_{Gi}(P_i)}{dP_i}\frac{dP_i}{d\rho} \\ &= P_i + \rho \frac{\partial (D - \sum_{j \neq i} P_j)}{\partial \rho} - C'_{Gi}(P_i)\frac{\partial (D - \sum_{j \neq i} P_j)}{\partial \rho} \\ &= 0 \end{aligned} \tag{6.14}$$

Combining and factoring out the partial derivative terms:

$$P_i + (\rho - C'_{Gi}(P_i)) \left[ \frac{\partial D}{\partial \rho} - \sum_{j \neq i} \frac{dP_j}{d\rho} \right] = 0 \tag{6.15}$$

Therefore, the profit maximization function for GenCo $i$ as a function $\rho$ is:

$$P_i = (\rho - C'_{Gi}(P_i)) \left[ -\frac{\partial D}{\partial \rho} + \sum_{j \neq i} \frac{dP_j}{d\rho} \right] \tag{6.16}$$

In order to get a more explicit expression for the optimal bid, this analysis

assumes that the demand is a linear function of the price:

$$D(\rho) = \frac{g}{d} - \frac{1}{d}\rho \tag{6.17}$$

and that Eq. 6.12 holds true because the system is lossless. Solving for $\rho$ and combining with Eq. 6.11 yields the inverse demand function:

$$\rho = g - d\sum_{j=1}^{N_G} P_i(\rho) \tag{6.18}$$

The inverse demand function is valuable because it jointly expresses the spot price $\rho$ as a function of the GenCo supply functions $P_i(\rho)$. The marginal cost for GenCo $i$ is maximized when:

$$\rho = g - d\sum_{j=1}^{N_G} P_i(\rho) \tag{6.19}$$

## 6.6 Bidding Analysis with Water-Fuel Costs

The IL200 will be used to assess the changes in market power with the water-fuel cost factored in. The breakdown of the state into 5 GenCos is shown in Fig. 6.5, and aggregate-level GenCo data is in Table 6.1. A detailed breakdown of each GenCo's individual power plants and cooling technologies is listed in Appendix B.

Table 6.1: IL200 Aggregate GenCo Data: Base Case.

| **GenCo** | **Capacity (MW)** | **Peak Demand (MW)** |
|---|---|---|
| 1 | 15591 | 17123 |
| 2 | 3451 | 1290 |
| 3 | 12866 | 2190 |
| 4 | 6410 | 1658 |
| 5 | 12170 | 1129 |

To demonstrate the details of bidding strategies, this example analysis will be performed from the perspective of GenCo1, a territory designed to represent PJM.

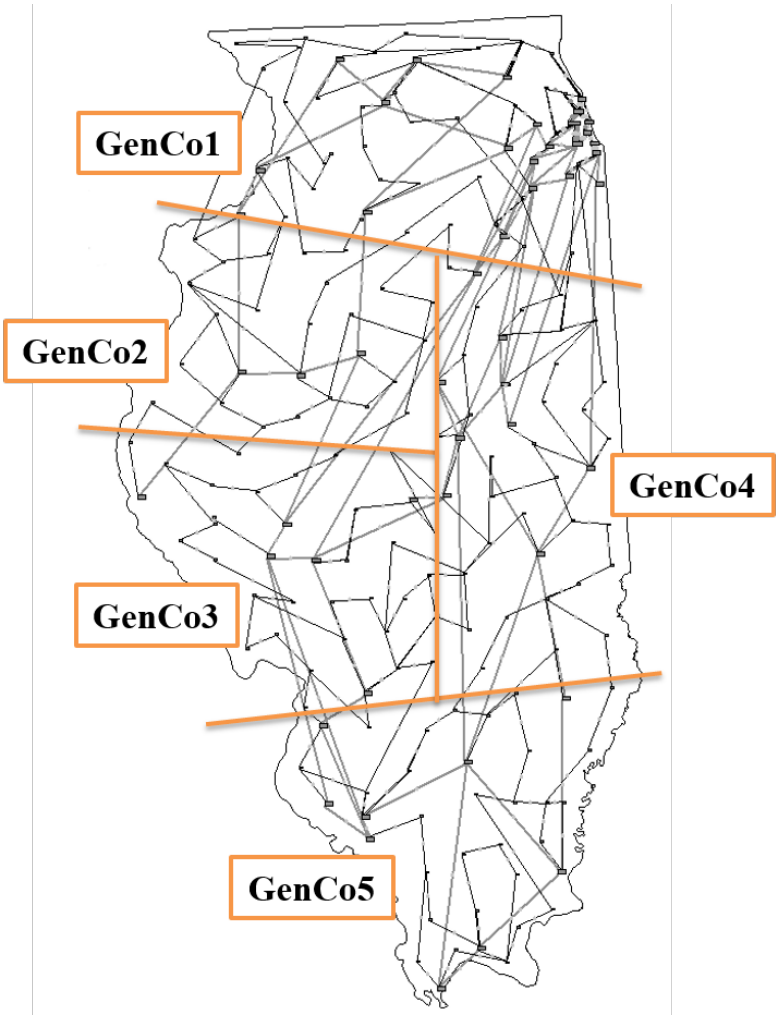


Figure 6.5: Division of the IL200 case to create generation companies.

Table 6.2: IL200 GenCo Cost Functions

| **GenCo** | $a_i$ (\$/h) | $b_i$ (\$/MWh) | $c_i$ (\$/MW$^2$h) |
|---|---|---|---|
| 1 | 1200 | 7 | 0.009 |
| 2 | 800 | 5 | 0.0086 |
| 3 | 500 | 4 | 0.015 |
| 4 | 650 | 6 | 0.007 |
| 5 | 875 | 5 | 0.002 |

Each GenCo's global marginal cost function is derived as in Section 6.5.1, with the resulting cost coefficients shown in Table 6.2. To incorporate the effects of the water cost, parameter $b_w$ is included in each generator's quadratic

cost:

$$C_i(P) = a_i + (b_i + b_w)P + c_i P^2 \tag{6.20}$$

The resulting cost coefficients for GenCo1, both with and without the water costs factored in, are shown in Fig. 6.6 and defined in Eq. 6.18. With the coefficients for the aggregate GenCo function known, the marginal cost curves for the PJM region before and after adding $b_w$ can be calculated; these curves are shown in Fig. 6.7.

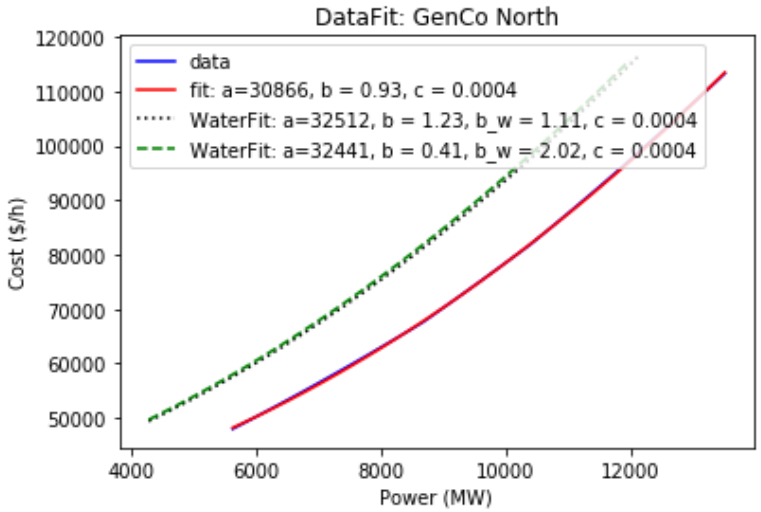


Figure 6.6: Creation of GenCo1's aggregate cost function with and without the water cost $b_w$.

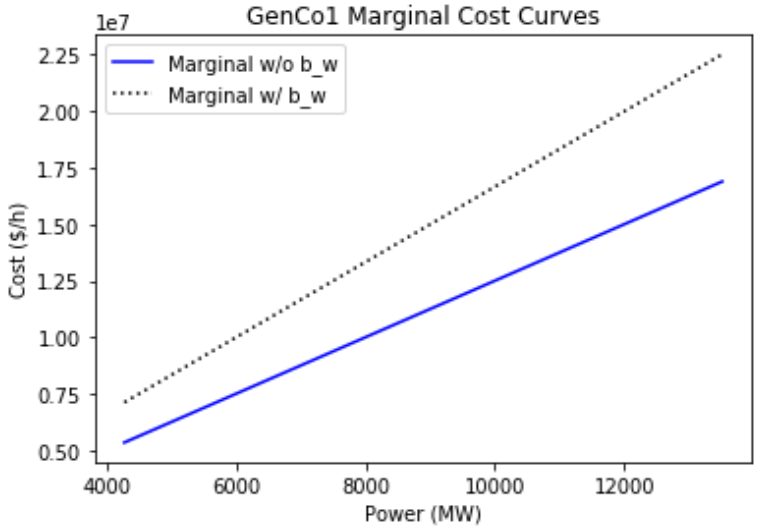


Figure 6.7: Marginal cost curves with and without $b_w$.

To create the linear demand function, PJM day-ahead price and demand data were fit to a linear curve in order to solve for $g$ and $d$, as shown in Fig. 6.8.

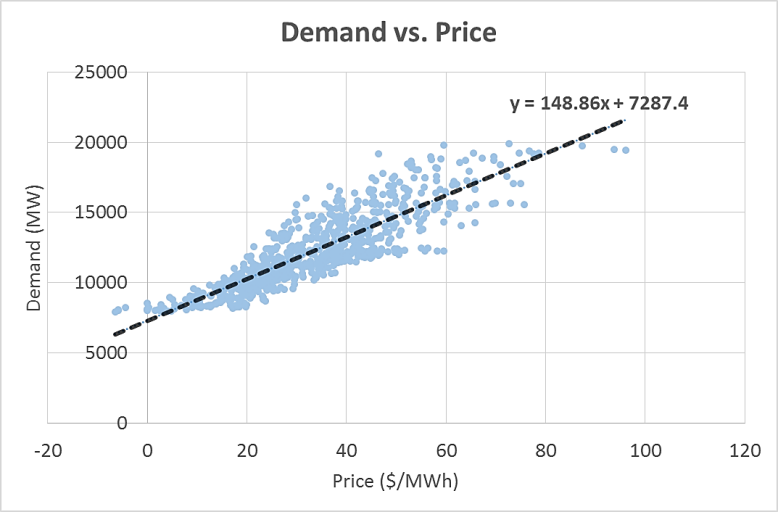


Figure 6.8: Linear fit of PJM load and price data for a summer month.

Solving for $g$ and $d$ yielded values:

$$g = 0.0067 \ \ \$/\text{MW}^2\text{h}$$
$$d = 42.83 \ \ \$/\text{MWh}$$

While this gives a linear demand function for the PJM system, in order to assess bidding strategies within the entire state, a demand for the entire state of Illinois is needed. Unfortunately MISO, the RTO who covers the rest of the state of Illinois (shown in Fig. 6.9) does not have price and demand data at the resolution of PJM. Approximations, however, can be made by using estimations calculated at the State Utility Forecasting Group (SUFG) at Purdue University [90].

For the purposes of MISO regional identification, the Illinois portion of their territory is referred to as *local resource zone (LRZ) 4*. According to the demand analysis for LRZ in the summer, an linear demand forecasting function was developed. Unlike the inverse demand function, which is a function of the price, the load forecasting factor $LF$ developed by the SUFG is a function of air temperature $T$:

$$LF = 0.8957 - 0.0003335T \tag{6.21}$$


Figure 6.9: Territory of the Midcontinent Independent System Operator (MISO).

The MISO data and line-fitting of load-factor vs. temperature data is shown in Fig. 6.10 [91].

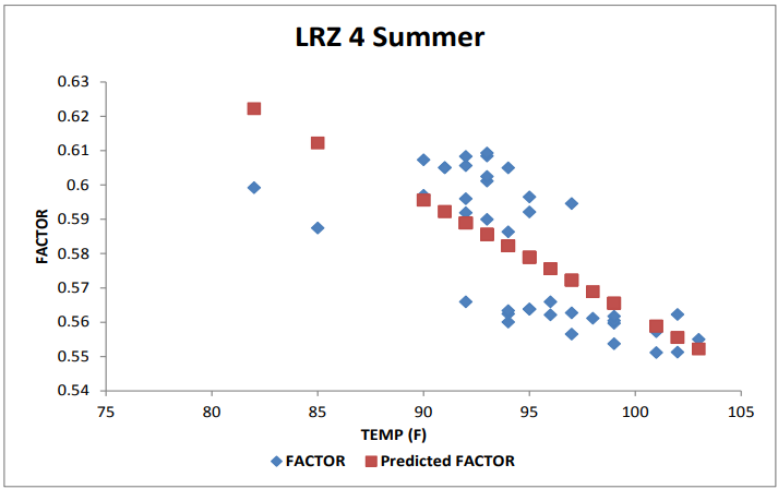


Figure 6.10: Curve-fitting of MISO summer load factor data.

Using temperature and peak demand data for the MISO region of Illinois, the LF calculation can be converted to a daily demand. To divide this region as in the IL200 GenCO divisions, the temperature for representative locations could be used as a load factor estimate. If historical MISO cost data were available as in the PJM region, a similar linear demand curve could be calculated for LRZ4 in order to determine $g$ and $d$ for GenCos 2-5.

## 6.7 Conclusions

This chapter outlined an additional application for the $b_w$ parameter, namely the potential for assessing changes in the MCP via GenCo-level supply-demand analysis. The calculation of the demand curve was demonstrated using PJM (i.e., ComEd) historical price and load data, and the supply curve was created via an aggregation of the individual generator data. Each unit had a $b_w$ parameter derived from its own plant configuration, and the aggregate level $b_w$ was calculated in order to get a sense for the GenCo's overall reliance on water across all cooling plants. The state level analysis could not be completed with the desired accuracy due to the unavailability of MISO price data.

Given that the water-cost is supposed to represent the dependence of generators on cooling water availability, and cooling water availability in the summer is not static, future work will look into the development of a $b_w$. The variable cost will be a penalty factor aimed at adjusting $b_w$ in situations where the water availability significantly changes. It is desirable to keep this cost tied to the individual generators (i.e., the plant configuration) experiencing this problem, rather than a sweeping cost increase across all generators.

# CHAPTER 7

# CONCLUSIONS AND FUTURE WORK

Past instances of cooling-water-driven deratings and shutdowns are already showing the effects of water availability on power system reliability and operations. The rise of research and funding opportunities within the water-energy nexus, as well as Department of Energy conferences, publications, and stakeholder meetings, all indicate that these water-availability issues are significant.

To address this problem, work needs to be done in developing models in which water and energy data can come together in order to drive policy and regulation at the state and federal levels. While there are advanced applications and tools available through national labs, they require environmental and energy data beyond what is available by generation companies. There are no straightforward techniques and parameters with which power-system operators and generation companies can analyze the effects of cooling water availability on their resiliency and operations.

To solve this problem, cooling-water-dependent parameters were proposed for use within electricity markets and reliability analysis. Through interdisciplinary work with civil engineers, thermoelectric cooling models were used to develop power plant derating parameters for reliability analysis. Additionally, a water-fuel cost parameter was inserted into deregulated electricity markets in order to calculate changes in revenue and bidding strategies, as well as determine changes in GenCo profits through asset valuation.

On the reliability side, the next steps involve further detailing the thermodynamics used within the power output maximization. Given that the original model was developed in order to maintain a system operating point, the model becomes unstable when power plant parameters are too far away from the original operating point.

Additionally, there have been instances where generation units along a common stream of water were close enough for the heat from one unit's dis-

charge to appear at the intake of the other. In other cases, a senior water rights holder can induce curtailment of a junior water rights holder through "first come, first served" prior appropriation water rights. For further reliability analysis, the co-dependency between generation units along a common body of water will be correlated. This quantification of their shared water use will be added to current risk and resiliency metrics to determine water's role in generation adequacy and system capacity.

Another project involves deeper analysis within the planning time-scales. The reliability metrics developed in Chapter 5 play a significant role in assessing planning alternatives since the probabilistic indices give long-term projections for system parameters. For example, the long-term streamflows and temperatures can be converted into derated generation operating points. This derating may suggest, after doing the planning assessment, that a renewable energy project may be more appealing than a recirculating steam plant due to water availability projections.

Additionally, the state of Illinois has a Renewable Portfolio Standard (RPS) law-mandated through the Illinois Power Agency Act. According to this statute:

> A minimum percentage of each utility's total supply to serve the load of eligible retail customers... shall be generated from cost-effective renewable energy resources:... at least 10% by June 1, 2015; and increasing by at least 1.5% each year thereafter to at least 25% by June 1, 2025.

The Act additionally suggests the percentage of renewables that should come from wind and photovoltaic generation, the minimum duration of renewable contracts, and desired nameplate capacities.

Generation data such as Form EIA-860, which includes data on existing and planned solar and wind plants, provide a starting point for developing renewable-energy-based planning cases. Capital costs are also a part of form EIA-860, so the values from this data set can be used to create renewable penetrations for the state of Illinois that are consistent with the RPS requirements.

# APPENDIX A

# GENERATOR PARAMETERS BY PLANT CONFIGURATION

Table A.1: Generator Forced Outage Rates (FOR) [74]

| **Fuel Type** | **Prime Mover** | **Nameplate Capacity (MW)** | FOR |
|---|---|---|---|
| Coal | Steam Turbine | 1-99 | 6.18 |
| | | 100-199 | 5.62 |
| | | 200-299 | 8.26 |
| | | 300-399 | 9.72 |
| | | 400-599 | 6.56 |
| | | 600-799 | 5.41 |
| | | 800-999 | 5.6 |
| | | $\geq$ 1000 | 4.37 |
| Nuclear | Steam Turbine | 1-799 | 2.33 |
| | | 800-999 | 1.34 |
| | | $\geq$ 1000 | 2.76 |
| NGas | Steam Turbine | 1-99 | 6.18 |
| | | 100-199 | 5.62 |
| | | 200-299 | 8.26 |
| | | 300-399 | 9.72 |
| | | 400-599 | 6.56 |
| | | 600-799 | 5.41 |
| | | 800-999 | 5.6 |
| | | $\geq$ 1000 | 4.37 |
| | Gas Turbine | 1-19 | 76.9 |
| | | 20-49 | 49.66 |
| | | $\geq$ 50 | 29.66 |
| | Combined Cycle | All | 3.72 |
| Hydro | N/A | 1-29 | 15.59 |
| | | $\geq$ 30 | 4.31 |

Table A.2: Median Water Usage Factors, Non-Renewable Technologies (gal/MWh) [54]

| **Fuel** | **Cooling** | **Technology** | **Cons.** | **With.** |
|---|---|---|---|---|
| Nuclear | Tower | Generic | 672 | 1101 |
| | Once-Thr. | | 269 | 44350 |
| | Pond | | 610 | 7050 |
| Nat. Gas | Tower | Combined Cycle | 198 | 253 |
| | | Steam | 826 | 1203 |
| | | Combined Cycle w/ CCS | 378 | 496 |
| | Once-thr. | Combined Cycle | 100 | 11380 |
| | | Steam | 240 | 35000 |
| | Pond | Combined Cycle | 240 | 5950 |
| | Dry | Combined Cycle | 2 | 2 |
| | Inlet | Steam | 340 | 425 |
| Coal | Tower | Generic | 687 | 1005 |
| | | Subcritical | 471 | 531 |
| | | Supercritical | 493 | 609 |
| | | IGCC | 372 | 390 |
| | | Subcritical w/ CCS | 942 | 1277 |
| | | Supercritical w/ CCS | 846 | 1123 |
| | | IGCC with CCS | 540 | 586 |
| | Once-thr. | Generic | 250 | 36350 |
| | | Subcritical | 113 | 27088 |
| | | Supercritical | 103 | 22590 |
| | Pond | Generic | 545 | 12225 |
| | | Subcritical | 779 | 17914 |
| | | Supercritical | 42 | 15046 |

Table A.3: Median Water Usage Factors, Renewable Technologies (gal/MWh) [54]

| **Fuel** | **Cooling** | **Technology** | **Consump.** | **With.** |
|---|---|---|---|---|
| Biopower | Tower | Steam | 553 | 878 |
| | | Biogas | 235 | N/A |
| | Once-Thr. | Steam | 300 | 35000 |
| | Pond | | 390 | 450 |
| | Dry | Biogas | 35 | N/A |
| PV | N/A | Utility-Scale PV | 26 | N/A |
| Wind | N/A | Wind Turbine | 0 | |
| CSP | Tower | Trough | 865 | |
| | | Power Tower | 786 | |
| | | Fresnel | 1000 | |
| | Dry | Trough | 78 | |
| | | Power Tower | 26 | |
| | Hybrid | Trough | 338 | |
| | | Power Tower | 170 | |
| | N/A | Stirling | 5 | |
| Geothermal | Tower | Dry Steam | 1796 | |
| | | Flash (freshwater) | 10 | |
| | | Flash (geothermal fluid) | 2583 | |
| | | Binary | 3600 | |
| | | EGS | 4784 | |
| | Dry | Flash | 0 | |
| | | Binary | 135 | |
| | | EGS | 850 | |
| | Hybrid | Binary | 221 | |
| | | EGS | 1406 | |
| Hydropower | N/A | in-stream & reservoir | 4491 | |

# APPENDIX B

# IL200 GENERATOR DATA

Table B.1: IL-200: GenCo1's Units

| Unit | FuelType | Mover | GenA | GenB | GenC | Cooling |
|---|---|---|---|---|---|---|
| 1 | Nuclear | ST | 1100.24 | 9.8202 | 0.0002 | RC |
| 2 | Hydro | HY | 0.00 | 0.0000 | 0.0000 | NA |
| 3 | Hydro | HY | 0.00 | 0.0000 | 0.0000 | NA |
| 4 | Hydro | HY | 0.00 | 0.0000 | 0.0000 | NA |
| 5 | Coal | ST | 236.04 | 8.7963 | 0.0009 | RF |
| 6 | Natural Gas | CT | 659.55 | 9.0344 | 0.0008 | RN |
| 7 | Coal | ST | 236.24 | 8.7963 | 0.0009 | RF |
| 8 | Natural Gas | CA | 1052.25 | 9.7198 | 0.0008 | OF |
| 9 | Natural Gas | CA | 852.00 | 9.3703 | 0.0008 | RI |
| 10 | Wind | WT | 0.00 | 0.0000 | 0.0000 | NA |
| 11 | Natural Gas | CA | 1052.25 | 9.7198 | 0.0008 | RI |
| 12 | Coal | ST | 236.53 | 8.7963 | 0.0009 | RF |
| 13 | Wind | WT | 0.00 | 0.0000 | 0.0000 | NA |
| 14 | Wind | WT | 0.00 | 0.0000 | 0.0000 | NA |
| 15 | Wind | WT | 0.00 | 0.0000 | 0.0000 | NA |
| 16 | Wind | WT | 0.00 | 0.0000 | 0.0000 | NA |
| 17 | Wind | WT | 0.00 | 0.0000 | 0.0000 | NA |
| 18 | Wind | WT | 0.00 | 0.0000 | 0.0000 | NA |
| 19 | Wind | WT | 0.00 | 0.0000 | 0.0000 | NA |
| 20 | Wind | WT | 0.00 | 0.0000 | 0.0000 | NA |
| 21 | Natural Gas | CA | 822.25 | 8.7198 | 0.0008 | RI |
| 22 | Wind | WT | 0.00 | 0.0000 | 0.0000 | NA |
| 23 | Wind | WT | 0.00 | 0.0000 | 0.0000 | NA |
| 24 | Wind | WT | 0.00 | 0.0000 | 0.0000 | NA |
| 25 | Coal | ST | 1069.79 | 8.7963 | 0.0009 | RI |

Table B.1: IL-200: GenCo1's Units (continued)

| Unit | FuelType | Mover | GenA | GenB | GenC | Cooling |
|---|---|---|---|---|---|---|
| 26 | Natural Gas | IC | 613.95 | 8.9548 | 0.0008 | NA |
| 27 | Natural Gas | IC | 602.40 | 8.9347 | 0.0008 | NA |
| 28 | Hydro | HY | 0.00 | 0.0000 | 0.0000 | NA |
| 29 | Wind | WT | 0.00 | 0.0000 | 0.0000 | NA |
| 30 | Hydro | HY | 0.00 | 0.0000 | 0.0000 | NA |
| 31 | Hydro | HY | 0.00 | 0.0000 | 0.0000 | NA |
| 32 | Wind | WT | 0.00 | 0.0000 | 0.0000 | NA |
| 33 | Nuclear | ST | 1270.38 | 9.0420 | 0.0002 | OC |
| 34 | Nuclear | ST | 1309.94 | 5.6066 | 0.0002 | RC |
| 35 | Nuclear | ST | 1274.49 | 6.2015 | 0.0002 | OF |
| 36 | Nuclear | ST | 1057.49 | 7.7713 | 0.0002 | RN |
| 37 | Natural Gas | CT | 852.57 | 10.0182 | 0.0008 | RN |
| 38 | Natural Gas | GT | 619.20 | 8.9640 | 0.0008 | NA |
| 39 | Natural Gas | GT | 618.60 | 8.9630 | 0.0008 | NA |
| 40 | Natural Gas | CT | 3859.00 | 10.5305 | 0.0008 | RN |
| 41 | Coal | ST | 1325.46 | 8.7963 | 0.0009 | OF |

Table B.2: IL-200: GenCo2's Units

| Unit | FuelType | Mover | GenA | GenB | GenC | Cooling |
|---|---|---|---|---|---|---|
| 1 | Coal | ST | 1258.62 | 8.7963 | 0.0009 | RF |
| 2 | Coal | ST | 1282.19 | 8.7963 | 0.0009 | RF |
| 3 | Natural Gas | IC | 616.95 | 8.9601 | 0.0008 | NA |
| 4 | Natural Gas | IC | 807.90 | 9.2933 | 0.0008 | NA |
| 5 | Coal | ST | 236.71 | 8.7963 | 0.0009 | RF |
| 6 | Coal | ST | 236.47 | 8.7963 | 0.0009 | RF |
| 7 | Coal | ST | 236.14 | 8.7963 | 0.0009 | RF |
| 8 | Coal | ST | 1347.27 | 8.7963 | 0.0009 | OF |
| 9 | Natural Gas | IC | 607.20 | 8.9431 | 0.0008 | NA |
| 10 | Natural Gas | IC | 606.30 | 8.9415 | 0.0008 | NA |
| 11 | Coal | ST | 236.48 | 8.7963 | 0.0009 | RF |
| 12 | Natural Gas | IC | 615.60 | 8.9577 | 0.0008 | NA |
| 13 | Natural Gas | IC | 852.00 | 9.3703 | 0.0008 | NA |
| 14 | Natural Gas | GT | 1074.00 | 9.7577 | 0.0008 | NA |

Table B.2: IL-200: GenCo2's Units (continued)

| Unit | FuelType | Mover | GenA | GenB | GenC | Cooling |
|---|---|---|---|---|---|---|
| 15 | Natural Gas | GT | 3859.00 | 11.0624 | 0.0008 | NA |
| 16 | Natural Gas | IC | 606.90 | 8.9425 | 0.0008 | NA |
| 17 | Natural Gas | IC | 606.60 | 8.9420 | 0.0008 | NA |
| 18 | Wind | WT | 0.00 | 0.0000 | 0.0000 | NA |
| 19 | Wind | WT | 0.00 | 0.0000 | 0.0000 | NA |
| 20 | Natural Gas | IC | 656.85 | 9.0297 | 0.0008 | NA |
| 21 | Coal | ST | 1110.74 | 8.7963 | 0.0009 | OF |

Table B.3: IL-200: GenCo3's Units

| Unit | FuelType | Mover | GenA | GenB | GenC | Cooling |
|---|---|---|---|---|---|---|
| 1 | Wind | WT | 0.00 | 0.0000 | 0.0000 | NA |
| 2 | Wind | WT | 0.00 | 0.0000 | 0.0000 | NA |
| 3 | Natural Gas | ST | 717.00 | 9.1347 | 0.0008 | OF |
| 4 | Natural Gas | ST | 606.60 | 8.9420 | 0.0008 | OF |
| 5 | Natural Gas | IC | 605.40 | 8.9399 | 0.0008 | NA |
| 6 | Natural Gas | ST | 609.00 | 8.9462 | 0.0008 | OF |
| 7 | Coal | ST | 236.89 | 8.7963 | 0.0009 | RI |
| 8 | Natural Gas | GT | 621.00 | 8.9672 | 0.0008 | NA |
| 9 | Natural Gas | GT | 610.50 | 8.9488 | 0.0008 | NA |
| 10 | Natural Gas | GT | 1005.00 | 9.6373 | 0.0008 | NA |
| 11 | Natural Gas | GT | 1512.52 | 10.1242 | 0.0008 | NA |
| 12 | Coal | ST | 236.14 | 8.7963 | 0.0009 | RI |
| 13 | Coal | ST | 236.10 | 8.7963 | 0.0009 | RI |
| 14 | Coal | ST | 236.24 | 8.7963 | 0.0009 | RI |
| 15 | Coal | ST | 236.10 | 8.7963 | 0.0009 | RI |
| 16 | Natural Gas | IC | 626.10 | 8.9342 | 0.0008 | NA |
| 17 | Natural Gas | IC | 606.60 | 8.9420 | 0.0008 | NA |
| 18 | Coal | ST | 1288.26 | 8.7963 | 0.0009 | OF |
| 19 | Coal | ST | 236.33 | 8.7963 | 0.0009 | RN |
| 20 | Coal | ST | 236.45 | 8.7963 | 0.0009 | RN |
| 21 | Coal | ST | 236.20 | 8.7963 | 0.0009 | RN |
| 22 | Natural Gas | IC | 603.60 | 8.9368 | 0.0008 | NA |
| 23 | Natural Gas | GT | 3630.87 | 10.4645 | 0.0008 | NA |

Table B.3: IL-200: GenCo3's Units (continued)

| Unit | FuelType | Mover | GenA | GenB | GenC | Cooling |
|---|---|---|---|---|---|---|
| 24 | Natural Gas | GT | 607.20 | 8.9431 | 0.0008 | NA |
| 25 | Natural Gas | GT | 610.80 | 8.9494 | 0.0008 | NA |
| 26 | Natural Gas | GT | 644.25 | 9.0077 | 0.0008 | NA |
| 27 | Natural Gas | GT | 609.00 | 8.9462 | 0.0008 | NA |
| 28 | Natural Gas | GT | 2881.30 | 10.3441 | 0.0008 | NA |
| 29 | Natural Gas | GT | 602.70 | 8.9352 | 0.0008 | NA |
| 30 | Natural Gas | GT | 603.30 | 8.9363 | 0.0008 | NA |
| 31 | Natural Gas | GT | 3859.00 | 10.7684 | 0.0008 | NA |
| 32 | Natural Gas | ST | 787.50 | 9.2577 | 0.0008 | OF |
| 33 | Natural Gas | ST | 706.50 | 9.1164 | 0.0008 | OF |
| 34 | Coal | ST | 1541.60 | 8.7963 | 0.0009 | OC |
| 35 | Natural Gas | GT | 612.45 | 8.9522 | 0.0008 | NA |
| 36 | Natural Gas | GT | 607.05 | 8.9428 | 0.0008 | NA |
| 37 | Natural Gas | GT | 3859.00 | 12.2682 | 0.0008 | NA |
| 38 | Natural Gas | GT | 609.60 | 8.9473 | 0.0008 | NA |
| 39 | Natural Gas | GT | 602.25 | 8.9344 | 0.0008 | NA |
| 40 | Natural Gas | GT | 609.90 | 8.9478 | 0.0008 | NA |
| 41 | Natural Gas | ST | 630.00 | 8.9829 | 0.0008 | OF |
| 42 | Natural Gas | GT | 604.35 | 8.9381 | 0.0008 | NA |
| 43 | Coal | ST | 1337.54 | 8.7963 | 0.0009 | RN |
| 44 | Natural Gas | GT | 1134.00 | 9.8624 | 0.0008 | NA |
| 45 | Natural Gas | GT | 2881.30 | 10.3441 | 0.0008 | NA |
| 46 | Natural Gas | GT | 1113.00 | 9.8258 | 0.0008 | NA |
| 47 | Natural Gas | GT | 606.30 | 8.9415 | 0.0008 | NA |
| 48 | Natural Gas | GT | 605.25 | 8.9397 | 0.0008 | NA |
| 49 | Natural Gas | ST | 882.00 | 9.4226 | 0.0008 | RI |
| 50 | Natural Gas | GT | 606.60 | 8.9420 | 0.0008 | NA |
| 51 | Coal | ST | 236.48 | 8.7963 | 0.0009 | OC |
| 52 | Coal | ST | 1177.90 | 8.7963 | 0.0009 | RF |
| 53 | Natural Gas | ST | 607.20 | 8.9431 | 0.0008 | RI |
| 54 | Natural Gas | ST | 622.50 | 8.9698 | 0.0008 | RI |
| 55 | Natural Gas | ST | 602.40 | 8.9347 | 0.0008 | RI |
| 56 | Natural Gas | ST | 601.65 | 8.9334 | 0.0008 | RI |

Table B.3: IL-200: GenCo3's Units (continued)

| Unit | FuelType | Mover | GenA | GenB | GenC | Cooling |
|---|---|---|---|---|---|---|
| 57 | Coal | ST | 236.97 | 8.7963 | 0.0009 | OC |
| 58 | Natural Gas | IC | 1005.00 | 9.6373 | 0.0008 | NA |
| 59 | Coal | ST | 236.14 | 8.7963 | 0.0009 | OC |
| 60 | Coal | ST | 236.73 | 8.7963 | 0.0009 | OC |
| 61 | Natural Gas | IC | 616.95 | 8.9601 | 0.0008 | NA |
| 62 | Natural Gas | GT | 603.60 | 8.9368 | 0.0008 | NA |
| 63 | Coal | ST | 305.60 | 8.7963 | 0.0009 | OC |
| 64 | Natural Gas | GT | 3859.00 | 10.7211 | 0.0008 | NA |
| 65 | Natural Gas | IC | 654.00 | 9.0247 | 0.0008 | NA |
| 66 | Natural Gas | ST | 604.80 | 8.9389 | 0.0008 | OF |
| 67 | Coal | ST | 1428.74 | 8.7963 | 0.0009 | OF |
| 68 | Natural Gas | GT | 602.10 | 8.9342 | 0.0008 | NA |
| 69 | Natural Gas | GT | 601.50 | 8.9331 | 0.0008 | NA |
| 70 | Natural Gas | GT | 604.95 | 8.9391 | 0.0008 | NA |
| 71 | Natural Gas | GT | 604.50 | 8.9384 | 0.0008 | NA |
| 72 | Natural Gas | GT | 1069.20 | 9.7493 | 0.0008 | NA |
| 73 | Natural Gas | GT | 717.32 | 9.9965 | 0.0008 | NA |
| 74 | Coal | ST | 237.65 | 8.7963 | 0.0009 | OC |
| 75 | Coal | ST | 236.13 | 8.7963 | 0.0009 | OC |
| 76 | Coal | ST | 236.68 | 8.7963 | 0.0009 | OC |
| 77 | Coal | ST | 236.45 | 8.7963 | 0.0009 | OC |
| 78 | Coal | ST | 236.14 | 8.7963 | 0.0009 | OC |
| 79 | Natural Gas | GT | 1952.48 | 10.1949 | 0.0008 | NA |
| 80 | Natural Gas | IC | 604.80 | 8.9389 | 0.0008 | NA |
| 81 | Coal | ST | 1698.83 | 8.7963 | 0.0009 | RC |

Table B.4: IL-200: GenCo4's Units

| Unit | FuelType | Mover | GenA | GenB | GenC | Cooling |
|---|---|---|---|---|---|---|
| 1 | Natural Gas | CT | 757.00 | 9.2125 | 0.0008 | RN |
| 2 | Natural Gas | CT | 828.30 | 9.3289 | 0.0008 | OC |
| 3 | Natural Gas | CA | 828.30 | 9.3289 | 0.0008 | RC |
| 4 | Wind | WT | 0.00 | 0.0000 | 0.0000 | NA |
| 5 | Wind | WT | 0.00 | 0.0000 | 0.0000 | NA |

Table B.4: IL-200: GenCo4's Units (continued)

| Unit | FuelType | Mover | GenA | GenB | GenC | Cooling |
|---|---|---|---|---|---|---|
| 6 | Wind | WT | 0.00 | 0.0000 | 0.0000 | NA |
| 7 | Wind | WT | 0.00 | 0.0000 | 0.0000 | NA |
| 8 | Wind | WT | 0.00 | 0.0000 | 0.0000 | NA |
| 9 | Nuclear | ST | 1233.74 | 8.0893 | 0.0002 | RC |
| 10 | Natural Gas | CA | 615.90 | 8.9583 | 0.0008 | RC |
| 11 | Natural Gas | GT | 604.80 | 8.9389 | 0.0008 | NA |
| 12 | Natural Gas | GT | 605.40 | 8.9399 | 0.0008 | NA |
| 13 | Natural Gas | GT | 605.25 | 8.9397 | 0.0008 | NA |
| 14 | Natural Gas | CA | 681.90 | 9.0734 | 0.0008 | RC |
| 15 | Natural Gas | GT | 607.50 | 8.9436 | 0.0008 | NA |
| 16 | Natural Gas | GT | 605.25 | 8.9397 | 0.0008 | NA |
| 17 | Natural Gas | GT | 601.80 | 8.9336 | 0.0008 | NA |
| 18 | Natural Gas | GT | 604.80 | 8.9389 | 0.0008 | NA |
| 19 | Natural Gas | CT | 689.85 | 9.0873 | 0.0008 | RN |
| 20 | Natural Gas | GT | 920.90 | 9.2933 | 0.0008 | NA |
| 21 | Natural Gas | IC | 611.10 | 8.9499 | 0.0008 | NA |
| 22 | Natural Gas | IC | 613.95 | 8.9549 | 0.0008 | NA |
| 23 | Natural Gas | IC | 602.40 | 8.9347 | 0.0008 | NA |
| 24 | Natural Gas | IC | 603.60 | 8.9368 | 0.0008 | NA |
| 25 | Natural Gas | IC | 602.55 | 8.9350 | 0.0008 | NA |
| 26 | Coal | ST | 236.19 | 8.7963 | 0.0009 | RI |
| 27 | Coal | ST | 1656.61 | 8.7963 | 0.0009 | OC |
| 28 | Natural Gas | GT | 607.50 | 8.9436 | 0.0008 | NA |
| 29 | Natural Gas | CA | 648.60 | 9.0153 | 0.0008 | RC |
| 30 | Natural Gas | GT | 3859.00 | 10.5305 | 0.0008 | NA |
| 31 | Natural Gas | IC | 606.60 | 8.9420 | 0.0008 | NA |
| 32 | Coal | ST | 236.09 | 8.7963 | 0.0009 | RI |
| 33 | Natural Gas | CT | 713.40 | 9.1284 | 0.0008 | RN |
| 34 | Natural Gas | GT | 606.00 | 8.9410 | 0.0008 | NA |
| 35 | Coal | ST | 1932.77 | 8.7963 | 0.0009 | RC |

Table B.5: IL-200: GenCo5's Units

| Unit | FuelType | Mover | GenA | GenB | GenC | Cooling |
|---|---|---|---|---|---|---|
| 1 | Natural Gas | CA | 623.95 | 8.9548 | 0.0008 | RC |
| 2 | Natural Gas | CT | 602.40 | 8.9347 | 0.0008 | OC |
| 3 | Coal | ST | 1987.17 | 8.7963 | 0.0009 | RC |
| 4 | Coal | ST | 236.40 | 8.7963 | 0.0009 | RI |
| 5 | Coal | ST | 236.81 | 8.7963 | 0.0009 | RI |
| 6 | Natural Gas | CT | 1170.00 | 9.9253 | 0.0008 | RC |
| 7 | Natural Gas | GT | 3859.00 | 10.6082 | 0.0008 | NA |
| 8 | Coal | ST | 1588.93 | 8.7963 | 0.0009 | OF |
| 9 | Natural Gas | GT | 1052.25 | 9.7198 | 0.0008 | NA |
| 10 | Coal | ST | 1249.10 | 8.7963 | 0.0009 | RI |
| 11 | Coal | ST | 236.14 | 8.7963 | 0.0009 | RI |
| 12 | Natural Gas | CT | 609.00 | 8.9462 | 0.0008 | RN |
| 13 | Natural Gas | CT | 607.05 | 8.9428 | 0.0008 | OC |
| 14 | Coal | ST | 236.64 | 8.7963 | 0.0009 | RN |
| 15 | Coal | ST | 236.42 | 8.7963 | 0.0009 | RN |
| 16 | Coal | ST | 1922.94 | 8.7963 | 0.0009 | OF |
| 17 | Natural Gas | CA | 603.30 | 8.9363 | 0.0008 | RC |
| 18 | Natural Gas | CA | 868.50 | 9.3991 | 0.0008 | RC |
| 19 | Natural Gas | GT | 3859.00 | 12.2184 | 0.0008 | NA |
| 20 | Natural Gas | GT | 3859.00 | 13.4540 | 0.0008 | NA |
| 21 | Natural Gas | IC | 602.10 | 8.9342 | 0.0008 | NA |
| 22 | Natural Gas | GT | 3859.00 | 10.7420 | 0.0008 | NA |
| 23 | Coal | ST | 1218.21 | 8.7963 | 0.0009 | OF |
| 24 | Coal | ST | 1699.33 | 8.7963 | 0.0009 | OF |

# APPENDIX C

# AUTOMATING SYSTEM ANALYSIS USING POWERWORLD SIMULATOR

## C.1 Introduction

In order to create the water variables, key generator parameters needed to be exported from PowerWorld. Based upon each unit's plant configuration (i.e., fuel, prime mover, and cooling type) and water usage factors obtained from external sources, the water-fuel cost $b_w$ is calculated for each generator.

Given that the work used a state-level system and various volume-based water costs, there was a lot of data to work with for each experiment. The developed water-dependent variables do not exist within current power system analysis techniques and, depending on the power systems software used, may require additional steps (manual or otherwise) to keep them connected to their respective test cases.

Additionally, there is a computational burden associated with moving and editing these data for every iteration of the market analysis. PBUC calculations are made for each generator, compared to hourly demand, and used to determine the commitment schedule. Depending on the number of days being simulated, the amount of time this takes can add up.

Fortunately, PowerWorld simulator has tools that assist with both the storing of additional system information and the automation of many analysis tasks. This appendix outlines the ways in which PowerWorld has facilitated this research through easy access to the profit results derived from $b_w$, creation/storage of custom variables, and externally accessing PowerWorld tools and functions via their COM interface [92]. $B7OPF$, a publicly-available PowerWorld training case, will be used to outline the PowerWorld tools as applied in this work.

## C.2 Water-Fuel Cost

### C.2.1 Generator Cost Function

The generator cost model as defined in PowerWorld is:

$$C_i(P_i) = f_i + \left[a_i + b_i P_i + c_i P_i^2 + d_i P_i^3\right] * f_c + V_{O\&M} P_i \tag{C.1}$$

where $a_i, b_i, c_i, d_i$ are the cubic function's cost coefficients; $f_c$ is the fuel cost [\$/MBtu]; $V_{O\&M}$ is the variable O&M cost [\$/MWh]; $P_i$ is the output power [MW]; and $f_i$ is an fuel-independent cost parameter.

PowerWorld allows the user to further manipulate cost functions via Cost Shift and Cost Multiplier parameters. The addition of these parameters, as explained in their documentation, "allows you to easily apply a shift to the cost function for the purpose of assessing how variations in bids impact profit". For cost shift $C_S$ and cost multiplier $C_M$, the new cost function becomes:

$$\bar{C}_i(P_i) = [C_i(P_i) + C_S] * C_M \tag{C.2}$$

with $C_M$ unitless and $C_S$ in \$/MWh.

An advantage to using these cost parameters is the fact that PowerWorld has separate variables for the economic results with and without $C_S/C_M$. These *scaled* (with $C_S/C_M$) economic results, as shown in the last column of Fig. C.1, are readily available for comparative economic analysis.

| Number of Bus | Name of Bus | Area Name of Gen | ID | Cost Shift $/MWh | Cost Multiplier | Profit $/hr | Profit $/hr (Scaled) |
|---|---|---|---|---|---|---|---|
| 1 | Bus 1 | Top | 1 | 1.701 | 1.000 | -1465.16 | -1681.98 |
| 2 | Bus 2 | Top | 1 | 0.000 | 1.000 | -1726.68 | -1726.68 |
| 4 | Bus 4 | Top | 1 | 0.000 | 1.000 | 824.57 | 824.57 |
| 6 | Bus 6 | Left | 1 | 0.022 | 1.000 | 1492.58 | 1488.09 |
| 7 | Bus 7 | Right | 1 | 0.350 | 1.000 | 417.65 | 347.50 |

Figure C.1: PowerWorld with the Model Explorer set to show header captions, improving readability of parameters within PowerWorld.

By setting $C_S = b_w$, where $b_w$ is the water-fuel cost, a user can analyze (and save) the system profits with and without the water costs all in one case. This makes it easier to manipulate the data, especially when used alongside PowerWorld's COM interface. Figure C.2 shows the $C_S$ value (the final

column) for each generator, with each value being calculated as in Section 5.4.

| Fixed Cost(Mbtu/hr) | IOB | IOC | IOD | Fuel Cost | Variable O&M | Fuel Type | Unit Type | Cooling Type | Cost Shift $/MWh |
|---|---|---|---|---|---|---|---|---|---|
| 373.50 | 7.620 | 0.0020 | 0.00000 | 2.590 | 0.000 | Natural Gas | ST (Steam Turbine) | RC | 1.701 |
| 403.61 | 7.519 | 0.0014 | 0.00000 | 2.590 | 0.000 | Natural Gas | GT (Gas Turbine) | NA | 0.000 |
| 0.00 | 0.000 | 0.0000 | 0.00000 | 0.000 | 0.000 | Wind | WT (Wind Turbine) | NA | 0.000 |
| 388.93 | 7.573 | 0.0013 | 0.00000 | 1.000 | 0.000 | Nuclear | ST (Steam Turbine) | RN | 0.022 |
| 194.28 | 7.771 | 0.0019 | 0.00000 | 2.160 | 0.000 | Coal | ST (Steam Turbine) | OC | 0.350 |

Figure C.2: PowerWorld with the Model Explorer set to show header captions, improving readability of parameters within PowerWorld.

### C.2.2 Cooling Type Parameter

The consolidation of user-defined parameters can be done via PowerWorld's "Custom Fields and Expressions". Custom fields allow users to add (and save) additional parameters to system cases in order to easily differentiate between case studies using the same model.

In this work, a key parameter that is not otherwise defined in PowerWorld is the generator cooling type. Each unique power plant configuration is defined by a generator's fuel type, prime mover, and cooling type, as these three parameters result in different water consumption and withdrawal factors. While PowerWorld already provides fuel-type and prime-mover parameters (*GenFuelType* and *GenUnitType*, respectively), being able to store the cooling types within the case would allow external code to readily identify the plant's water usage factors.

In order to create this *GenCoolingType* custom field, a user needs to specify

- the number of variables used (one);
- the parameter's data type (string);
- the object this variable is used with ("Gen");
- the text to appear when hovering over the column ("Generator Cooling Code");
- the column header to use ("Cooling Type").

With the specifications outlined in the parentheses, the custom field would be defined in PowerWorld as in Fig. C.3.

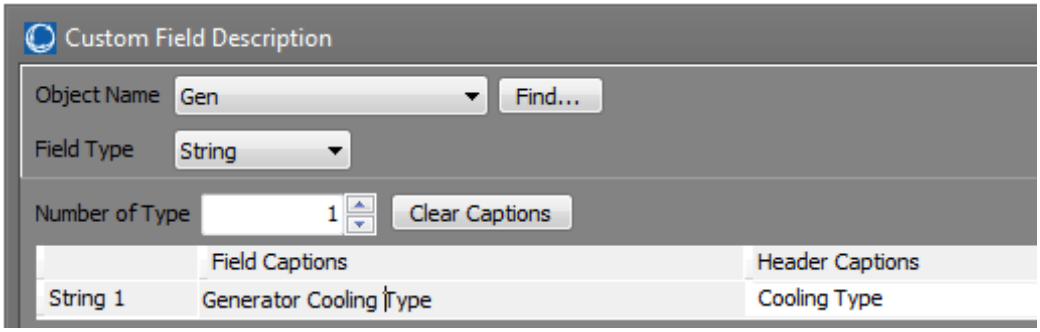


Figure C.3: Creating the cooling type parameter using PowerWorld's Custom Fields interface.

## C.3 Automation Server (SimAuto)

PowerWorld's Simulator Automation Server (SimAuto) provides developers of external programs with the functions, data manipulation tools, etc. used within PowerWorld. This allows users to automate much of their power system analysis, allowing them to focus on research and results [93]. Accessing PowerWorld functions and case data from a user-developed application is done using a COM Object, available through various Windows-based applications that have COM compatibility. The following code examples are all written in Python 2.7, the programming language used in this thesis work.

### C.3.1 Connecting and Opening a Case

```
# Import the COM functionality for SimAuto
import win32com
import pythoncom # This will import VT_VARIANT

# Connect to PowerWorld's COM server
SimAuto = win32com.client.Dispatch('pwrworld.SimulatorAuto')

# Open the B7OPF Case File
filename = 'C:/Users/TestUser/PWD/B7OPF.pwb'
Output = SimAuto.OpenCase(filename)
if Output[0] != '':
        print('Error: ' + Output[0])
```

This is the minimal coding required to connect to the PowerWorld COM server and open the B7OPF case: the user may want to specify a **try...else**

clause in order to capture COM errors or output success statements.

When making function calls via the SimAuto object (e.g., *SimAuto.OpenCase(filename)*), as shown in Fig. C.4, the object returned may be a tuple of size 2. The first item in the tuple will be an empty string unless an error occurred with the function call. If the call was successful and data was being exported via that function call, then the resulting data will be in the second item. The rows of the data store the same parameter for each object (e.g., all of the bus numbers for a group of generators).

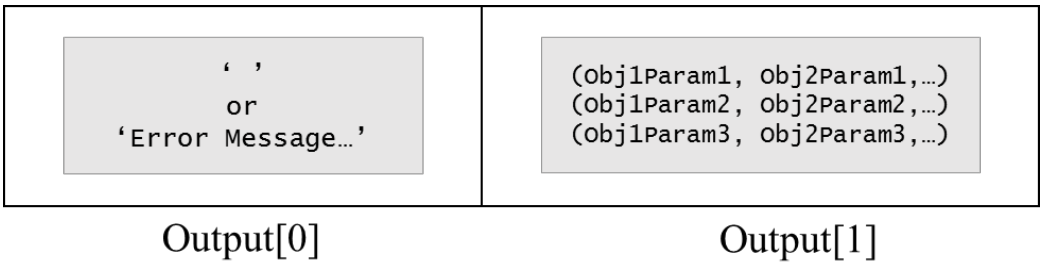


Figure C.4: Format of the SimAuto output array, of which there is two items.

### C.3.2 Manipulating Data

In order to edit/access system parameters via SimAuto, the case parameters (e.g., $a_i$, $b_i$) need to be referenced using their variable names. With PowerWorld Simulator's default settings, the column headers that appear in the Model Explorer are not the variable names. Figure C.5 shows the cost data for generators in the B7OPF case, with the bottom table displaying the corresponding variable names that would need to be called externally. Note that the custom cooling type parameter, defined as in Section C2.2, is called *CustomString*. To change these headers, access the "Options" via the Model Explorer window.

### C.3.3 Export Data from B7OPF

With the exact name of the $C_S$ parameter (*GenExtraOMCost*) identified, additional case data (including the custom cooling type variable) can be exported in order to convert each generator's plant configuration into a water cost.

| Fixed Cost(Mbtu/hr) | IOB | IOC | IOD | Fuel Cost | Variable O&M | Fuel Type | Unit Type | Cooling Type | Cost Shift $/MWh |
|---|---|---|---|---|---|---|---|---|---|
| 373.50 | 7.620 | 0.0020 | 0.00000 | 2.590 | 0.000 | Natural Gas | ST (Steam Turbine) | RC | 1.701 |
| 403.61 | 7.519 | 0.0014 | 0.00000 | 2.590 | 0.000 | Natural Gas | GT (Gas Turbine) | NA | 0.000 |
| 0.00 | 0.000 | 0.0000 | 0.00000 | 0.000 | 0.000 | Wind | WT (Wind Turbine) | NA | 0.000 |
| 388.93 | 7.573 | 0.0013 | 0.00000 | 1.000 | 0.000 | Nuclear | ST (Steam Turbine) | RN | 0.022 |
| 194.28 | 7.771 | 0.0019 | 0.00000 | 2.160 | 0.000 | Coal | ST (Steam Turbine) | OC | 0.350 |

| GenIOA | GenIOB | GenIOC | GenIOD | GenFuelCost | GenVariableOM | GenFuelType | GenUnitType | CustomString | GenExtraOMCost |
|---|---|---|---|---|---|---|---|---|---|
| 373.50 | 7.620 | 0.0020 | 0.00000 | 2.590 | 0.000 | Natural Gas | ST (Steam Turbine) | RC | 1.701 |
| 403.61 | 7.519 | 0.0014 | 0.00000 | 2.590 | 0.000 | Natural Gas | GT (Gas Turbine) | NA | 0.000 |
| 0.00 | 0.000 | 0.0000 | 0.00000 | 0.000 | 0.000 | Wind | WT (Wind Turbine) | NA | 0.000 |
| 388.93 | 7.573 | 0.0013 | 0.00000 | 1.000 | 0.000 | Nuclear | ST (Steam Turbine) | RN | 0.022 |
| 194.28 | 7.771 | 0.0019 | 0.00000 | 2.160 | 0.000 | Coal | ST (Steam Turbine) | OC | 0.350 |

Figure C.5: PowerWorld generator data with the Model Explorer set to show header (top) and variable (bottom) names.

```
# Import the COM functionality for SimAuto
GenFields = ['BusNum', 'GenID', 'GenFuelType', 'GenUnitType
    :1', 'CustomString']
FieldArray = VARIANT(pythoncom.VT_VARIANT | pythoncom.
    VT_ARRAY, GenFields)

# Grab the desired generator parameters
Output = SimAuto.GetParametersMultipleElement('GEN',
    FieldArray, '')
if Output[0] != '':
        print('Error: ' + Output[0])
else:
        GenData = Output[1]
        numGens = len(Output[1][0])
```

For the *GenUnitType* parameter, the ':1' refers to our desire to grab the two-character identifier instead of the full prime-mover name (e.g., 'ST' instead of 'Steam Turbine').

Once the data has been exported into the *GenData* object, a GetWaterCost function grabs the plant configuration data and creates *WaterCosts*, a 2D array where each row of data contains a generator's $BusNum$, $GenID$, and $b_w$, respectively.

### C.3.4 Import Data to B7OPF

With the $b_w$ costs calculated, $C_S$ (i.e.: *GenExtraOMCost*) can be specified for each generator in the B7OPF case. First, the variant object that will import the data is initialized.

```
# Initialize the water costs variant
GenFields = ['BusNum','GenID','GenExtraOMCost']
FieldArray = VARIANT(pythoncom.VT_VARIANT | pythoncom.
    VT_ARRAY, GenFields)
AllGensArray = [VARIANT(pythoncom.VT_VARIANT | pythoncom.
    VT_ARRAY, [None,None,None]) for i in range(numGens)]
```

From there, an iterative loop will run through each row of *WaterCosts* in order to set *GenExtraOMCost* in the variant array.

```
# Prepare the variant to import the cost shift parameter
gen_iter = 0
for BusNum, GenID, bWater in WaterCosts:
        AllGensArray[gen_iter].value = [BusNum, GenID,
            bWater]
        gen_iter += 1

# Update the B7OPF Case with cost shift b_w
Output = SimAuto.ChangeParametersMultipleElement('GEN',
    FieldArray, AllGensArray)
if Output[0] != '':
        print('Error: ' + Output[0])
else:
        print('Water costs added to B7OPF.')
```

### C.3.5 Run the OPF and Obtain the Profits

The only remaining steps are to run the OPF and export the profit data for further analysis.

```
# Solve the Primal LP
RunOPFcmd = 'SetData(Area, [BGAGC], ["OPF"], ALL); EnterMode
    (PowerFlow); SolvePrimalLp;'
Output = SimAuto.RunScriptCommand(RunOPFcmd)
if Output[0] != '':
        print('Error: ' + Output[0])
```

Profit data is obtained via variables *GenLMPProfitScaled* and *GenLMPProfitUnscaled*, the profits for each generator ($/h) with and without $b_w$, respectively.

```
# Profit parameters to export
```

```
ProfitFields = ['BusNum', 'GenLMPProfitUnscaled',
'GenLMPProfitScaled']
ProfitArray = VARIANT(pythoncom.VT_VARIANT | pythoncom.
    VT_ARRAY, ProfitFields)

# Grab the hourly profit data
Output = SimAuto.GetParametersMultipleElement('GEN',
    ProfitArray, '')
if Output[0] == '':
        ProfitData = Output[1]
else:
        print('Error: ' + Output[0])
```

# REFERENCES


[1] "Drought Impacts California's Energy: Governor Brown's Response Plan (Executive Order B-29-15)," 2015, California Energy Commission. [Online]. Available: http://www.energy.ca.gov/drought/

[2] "Water Use for Electricity Generation and Other Sectors: Recent Changes (1985-2005) and Future Projections (2005-2030)," Electric Power Research Institute, Tech. Rep., 2011.

[3] B. Carney, "Water Vulnerabilities for Existing Coal-fired Power Plants," National Energy Technology Laboratory, Tech. Rep. DOE/NETL-2010/1429, 2010.

[4] A. Mittal and M. Gaffigan, "Energy-Water Nexus: Improvements to Federal Water Use Data Would Increase Understanding of Trends in Power Plant Water Use," Government Accountability Office, Tech. Rep. GAO-10-23, 2009.

[5] A. Mittal and F. Rusco, "Energy-Water Nexus: Coordinated Federal Approach Needed to Better Manage Energy and Water Tradeoffs," Government Accountability Office, Tech. Rep. GAO-12-880, September 2012.

[6] "Current Opportunities Related to Water-Energy," June 2017, Department of Energy. [Online]. Available: https://www.energy.gov/under-secretary-science-and-energy/current-opportunities-related-water-energy

[7] "NSF Invests 72 Million in Innovations at Nexus of Food, Energy and Water Systems," September 2016, National Science Foundation. [Online]. Available: https://www.nsf.gov/news/news_summ.jsp?cntn_id=189898

[8] S. Acharya, B. Hamilton, and D. Reinhart, "Workshop Report: Developing a Research Agenda for the Energy Water Nexus," in *NSF Energy-Water Nexus Workshop*, December 2013.

[9] "A Water-Energy Research Agenda: Building California's Policy Foundation for the 21st Century," April 2014, Water in the West.

[10] "Addressing the Energy-Water Nexus: A Blueprint for Action and Policy Agenda," May 2011, Alliance for Water Efficiency.

[11] "Takeaways from the 2015 DOE Energy-Water Nexus Roundtable Series," 2015, Department of Energy. [Online]. Available: https://www.energy.gov/under-secretary-science-and-energy/downloads/energy-water-roundtables

[12] H. Battey, Z. Clement, F. Fields, and J. Li, "Water-Energy Nexus: Challenges and Opportunities," U.S. Department of Energy, Tech. Rep., 2014.

[13] B. Scanlon, I. Duncan, and R. Reedy, "Drought and the Water-Energy Nexus in Texas," *Environmental Research Letters*, vol. 8, no. 4, December 2013.

[14] "Texas Commission on Environmental Quality v. Texas Farm Bureau," 2015. [Online]. Available: https://s3.amazonaws.com/static.texastribune.org/media/documents/Opinion_--_TCEQ_v._Texas_Farm_Bureau_00826787x7A30F_1.pdf

[15] J. Malewitz, "In Major Water Case, Win for Ranchers is Loss For Cities," February 2016, The Texas Tribune. [Online]. Available: https://www.texastribune.org/2016/02/19/major-water-case-win-farmers-loss-cities/

[16] Peter Coy, "Making Water More Liquid," August 2015. [Online]. Available: https://www.bloomberg.com/news/articles/2015-08-06/to-ease-california-s-drought-make-water-easier-to-trade

[17] A. J. Wood, B. F. Wollenberg, and G. Sheblé, *Power Generation, Operation, and Control*. John Wiley & Sons, 2014.

[18] J. Maulbetsch and B. Barker, "Water Use for Electric Power Generation," Electric Power Research Institute, Tech. Rep. 1014026, 2008.

[19] "Water Properties: Facts and Figures about Water," December 2016, United States Geological Survey. [Online]. Available: https://water.usgs.gov/edu/water-facts.html

[20] P. Torcellini, N. Long, and R. Judkoff, "Consumptive Water Use for U.S. Power Production," National Renewable Energy Laboratory, Tech. Rep. TP-550-33905, December 2003.

[21] "Many Newer Power Plants Have Cooling Systems that Reuse Water," February 2014, Energy Information Administration. [Online]. Available: https://www.eia.gov/todayinenergy/detail.php?id=14971

[22] "Hydropower - Energy Explained," June 2017, Energy Information Administration. [Online]. Available: https://www.eia.gov/energyexplained/?page=hydropower_home

[23] "Hydropower Vision," July 2016. [Online]. Available: http://www1.eere.energy.gov/library/asset_handler.aspx?src=https://energy.gov/sites/prod/files/2016/10/f33/Hydropower-Vision-10262016_0.pdf&id=7496

[24] *Effluent Limitations Guidelines and Standards for the Steam Electric Power Generating Point Source Category*, Environmental Protection Agency, November 2015.

[25] "Federal Water Pollution Control Act (33 U.S.C. 1251 et seq.)," November 2002. [Online]. Available: https://www.epw.senate.gov/water.pdf

[26] J. McCall, J. Macknick, and D. Hillman, "Water-Related Power Plant Curtailments: An Overview of Incidents and Contribution Factors," National Renewable Energy Laboratory, Tech. Rep. TP-6A20-67084, 2016.

[27] "The Drought of 2012 - A Report of the Governor's Drought Response Task Force," March 2013, Illinois State Water Survey. [Online]. Available: http://www.isws.illinois.edu/hilites/drought/archive/2012/docs/TheDroughtOf2012.pdf

[28] D. Wagman, "Water Issues Challenge Power Generators," *Power Magazine*, July 2013. [Online]. Available: http://www.powermag.com/water-issues-challenge-power-generators/

[29] P. N. Davis, "Riparian Rights," in *Water Resources Allocation: Laws and Emerging Issues (Summer Conference, June 8-11)*, 1981.

[30] M. Davis, "A Toe in the Water: A Primer on Louisiana Riparian Law and Emerging Issues Prepared for the Louisiana Mineral Law Institute," March 2009, Tulane Institute on Water Resources Law and Policy. [Online]. Available: http://www.law.tulane.edu/uploadedFiles/Institutes_and_Centers/Water_Resources_Law_and_Policy/Content/A%20Toe%20in%20the%20Water,%20Davis%20,%20Mineral%20Law%20Inst.pdf

[31] "Water Laws and Policies for a Sustainable Future: A Western States Perspective," June 2008, Western States Water Council. [Online]. Available: http://www.westernstateswater.org/wp-content/uploads/2012/10/laws-policies-report-final-with-cover-1.pdf

[32] C. L. McGuinness, *Water Law With Special Reference to Ground Water*, United States Geological Survey, June 1951.

[33] "State Engineer Approves Applications to Use Green River Water for Nuclear Power Plant," 2016, State of Utah Department of Natural Resources. [Online]. Available: https://www.waterrights.utah.gov/pressRelease/greenRiverNuclearPowerPressRelease.pdf

[34] "HEAL Utah v. Kane County Water Conservancy District," July 2016, The Utah Court of Appeals. [Online]. Available: https://www.utcourts.gov/opinions/appopin/HEAL%20Utah%20v.%20Kane%20Co.%20Water%20Conservancy%20District20160721.pdf

[35] J. J. Peck and A. D. Smith, "Modeling Power Generation Water Usage," in *ASME 2015 Power Conference*, 2015.

[36] J. Macknick, E. Zhou, M. O'Connell, G. Brinkman, A. Miara, E. Ibanez, and M. Hummon, "Water and Climate Impacts on Power System Operations: The Importance of Cooling Systems and Demand Response Measures," National Renewable Energy Laboratory, Tech. Rep. TP-6A20-66714, December 2016.

[37] M. Wu and M. Peng, "Developing a Tool to Estimate Water Use in Electric Power Generation in the United States," Argonne National Laboratory, Tech. Rep. ANL/ESD/11-2, December 2010.

[38] C. Harto and E. Yan, "Analysis of Drought Impacts on Electricity Production in the Western and Texas Interconnections of the United States," Argonne National Library, Tech. Rep. ANL/EVS/R-11/14, 2011.

[39] D. X. Duc, J. G. Singh, and W. Ongsakul, "Water Valuation in Vietnamese Electric Power Generation Market," in *2011 International Conference Utility Exhibition on Power and Energy Systems: Issues and Prospects for Asia (ICUE)*, Sept 2011, pp. 1–7.

[40] A. Loew, P. Jaramillo, and H. Zhai, "Marginal Costs of Water Savings from Cooling System Retrofits: a Case Study for Texas Power Plants," *Environmental Research Letters*, vol. 11, no. 10, 2016.

[41] T. A. DeNooyer, J. M. Peschel, Z. Zhang, and A. S. Stillwell, "Integrating Water Resources and Power Generation: The EnergyWater Nexus in Illinois," *Applied Energy*, vol. 162, pp. 363 – 371, 2016.

[42] E. A. Martin and B. L. Ruddell, "Value Intensity of Water used for Electrical Energy Generation in the Western U.S.: An Application of Embedded Resource Accounting," in *2012 IEEE International Symposium on Sustainable Systems and Technology (ISSST)*, May 2012, pp. 1–5.

[43] C. Schaffner and X. P. Zhang, "Test systems for Economic Analysis An introduction," in *IEEE PES General Meeting*, July 2010, pp. 1–2.

[44] D. Krishnamurthy, W. Li, and L. Tesfatsion, "An 8-Zone Test System Based on ISO New England Data: Development and Application," *IEEE Transactions on Power Systems*, vol. 31, no. 1, pp. 234–246, Jan 2016.

[45] A. B. Birchfield, K. M. Gegner, T. Xu, K. S. Shetye, and T. J. Overbye, "Statistical Considerations in the Creation of Realistic Synthetic Power Grids for Geomagnetic Disturbance Studies," *IEEE Transactions on Power Systems*, vol. 32, no. 2, pp. 1502–1510, March 2017.

[46] T. Xu, A. B. Birchfield, K. M. Gegner, K. S. Shetye, and T. J. Overbye, "Application of Large-Scale Synthetic Power System Models for Energy Economic Studies," in *Hawaii International Conference on System Sciences (HICSS-50)*, 2017.

[47] D. Phillips, T. Xu, and T. Overbye, "Analysis of economic criteria in the creation of realistic synthetic power systems," in *2017 IEEE Manchester PowerTech*, June 2017, pp. 1–5.

[48] S. Stoft, *Power System Economics:Designing Markets for Electricity*. Wiley-IEEE Press, 2002, ch. 6, pp. 60–73.

[49] T. J. Overbye, Xu Cheng, and Yan Sun, "A comparison of the AC and DC power flow models for LMP calculations," in *37th Annual Hawaii International Conference on System Sciences, 2004. Proceedings of the*, Jan 2004.

[50] "LMP Consolidated Table," October 2016, Mid-continent Independent System Operator. [Online]. Available: https://www.misoenergy.org/MarketsOperations/RealTimeMarketData/Pages/LMPConsolidatedTable.aspx

[51] M. A. Maupin, J. F. Kenny, S. S. Hutson, J. K. Lovelace, N. L. Barber, and K. S. Linsey, "Estimated Use of Water in the United States in 2010: U.S. Geological Survey Circular 1405," United States Geological Survey, Tech. Rep. 1405, 2014.

[52] "Annual Electric Generator Data - EIA-860 Data File," US Energy Information Administration. [Online]. Available: https://www.eia.gov/electricity/data/eia860/

[53] "Annual Electricity Utility Data - EIA-906/920/923 Data File," US Energy Information Administration. [Online]. Available: https://www.eia.gov/electricity/data/eia923/

[54] J. Macknick, R. Newmark, G. Heath, and K. Hallett, "A Review of Operational Water Consumption and Withdrawal Factors for Electricity Generating Technologies," National Renewable Energy Laboratory, Tech. Rep. TP-6A20-50900, March 2011.

[55] A.-M. Fennell, "Freshwater: Supply Concerns Continue, and Uncertainties Complicate Planning," Government Accountability Office, Tech. Rep. GAO-14-430, 2014.

[56] M. Čepin, *Assessment of Power System Reliability: Methods and Applications*. Springer London, 2011.

[57] R. Billinton and R. Allan, *Generating CapacityBasic Probability Methods*. Springer US, 1996, pp. 18–82.

[58] Wenyuan Li, *Elements of Risk Evaluation Methods*. Wiley-IEEE Press, 2014, pp. 560–.

[59] R. Billinton and W. Li, *Reliability Assessment of Electric Power Systems Using Monte Carlo Methods*. Springer Science+Business Media, LLC, 1994.

[60] *IEEE Standard Definitions for Use in Reporting Electric Generating Unit Reliability, Availability, and Productivity*, IEEE Std 762-2006, March 2006.

[61] W. Lubega and A. Stillwell, "Maintaining Electric Grid Reliability under Hydrologic Drought and Heat Wave Conditions," *Applied Energy*, 2017.

[62] M. P. Berkenpas, K. Kietzke, S. T. McCoy, and E. Rubin, "IECM Technical Documentation Updates Report," Carnegie Mellon University, Tech. Rep., 2009.

[63] M. J. Rutberg, A. Delgado, H. J. Herzog, and A. Ghoniem, "A System-Level Generic Model of Water Use at Power Plants and its Application to Regional Water Use Estimation," in *ASME 2011 International Mechanical Engineering Congress and Exposition*, vol. 1, 01 2011.

[64] "Average Tested Heat Rates by Prime Mover and Energy Source, 2007 - 2015," Energy Information Administration. [Online]. Available: https://www.eia.gov/electricity/annual/html/epa_08_02.html

[65] "Illinois Environmental Protection Agency, NPDES Permit No. IL0001970," 2013.

[66] "Illinois Environmental Protection Agency, NPDES Permit No. IL0002216," 2012.

[67] "Illinois Environmental Protection Agency, NPDES Permit No. IL0064254," 2016.

[68] "Illinois Environmental Protection Agency, NPDES Permit No. IL0002208," 2013.

[69] J. Edinger and J. Geyer, *Heat Exchange in the Environment: A Study of the Physical Principles Relating to Power Plant Condenser Cooling Water Discharges*, ser. Cooling water studies for Edison Electric Institute Research Project RP-49. Edison Electric Institute, 1965.

[70] L. Benyahya, D. Caissie, A. St Hilaire, T. B. Ouarda, and B. Bobée, "A Review of Statistical Water Temperature Models," *Canadian Water Resources Journal / Revue canadienne des ressources hydriques*, vol. 32, no. 3, pp. 179–192, 2007.

[71] "Illinois State Climatologist Data," 2014, Illinois State Water Survey. [Online]. Available: www.isws.illinois.edu/atmos/statecli

[72] "The Drought of 2012 - A Report of the Governor's Drought Response Task Force," Illinois Department of Natural Resources, Tech. Rep., 2013.

[73] K. Kunkel, J. Angel, S. Changnon, R. Claybrooke, S. Hilberg, V. Knapp, R. Larson, M. Palecki, R. Scott, and D. Winstanley, "The 2005 Illinois Drought," Illinois State Water Survey, Tech. Rep., 2006.

[74] "GADS data reporting instructions," January 2017, North American Electric Reliability Corporation. [Online]. Available: http://www.nerc.com/pa/RAPA/gads/DataReportingInstructions/Appendix_F\%20-\%20Equations.pdf

[75] A. Morris, "Lessons from the Development of Western Water Law for Emerging Water Markets: Common Law vs Central Planning," *Oregon Law Review*, 2001.

[76] B. K. Pokharel, G. B. Shrestha, T. T. Lie, and S. E. Fleten, "Price based unit commitment for Gencos in deregulated markets," in *IEEE Power Engineering Society General Meeting, 2005*, June 2005, pp. 428–433 Vol. 1.

[77] B. Baker, "Running Dry at the Power Plant," *EPRI Journal 2007*, no. 1, pp. 26–35, 2007.

[78] "Consolidated Water (CWCO) Profit Margin History," 2017, Macro Trends. [Online]. Available: http://www.macrotrends.net/stocks/charts/CWCO/profit-margin/consoltd-water-gross-operating-net-profit-margin-history

[79] "Margin by Sector (US)," January 2017, NYU Stern School of Business. [Online]. Available: http://pages.stern.nyu.edu/~adamodar/New_Home_Page/datafile/margin.html

[80] "PJM - Territory Served," April 2018, PJM Interconnection. [Online]. Available: http://www.pjm.com/-/media/about-pjm/pjm-zones.ashx?la=en

[81] "PJM - Energy Market," PJM Interconnection. [Online]. Available: http://www.pjm.com/markets-and-operations/energy.aspx

[82] "Recent Rainfall, Drought, and Southern Australia's Long-Term Rainfall Decline," April 2015, Bureau of Meteorology. [Online]. Available: http://www.bom.gov.au/climate/updates/articles/a010-southern-rainfall-decline.shtml

[83] G. Rothwell and T. Gòmez, *Electricity Regulation and Deregulation*. Wiley-IEEE Press, 2003, pp. 1–13.

[84] M. Shahidehpour, H. Yamin, and Z. Li, *Market Operations in Electric Power Systems: Forcasting, Scheduling and Risk Management*. John Wiley & Sons, 2002.

[85] L. Tesfatsion, "Auction basics for wholesale power markets: Objectives and pricing rules," in *2009 IEEE Power Energy Society General Meeting*, July 2009, pp. 1–8.

[86] K. Leyton Brown and Y. Shoham, *Essentials of Game Theory*, R. Brachman and T. Dietterich, Eds. Morgan & Claypool, 2008.

[87] A. Maiorano, Yong-Hua Song, and M. Trovato, "Modelling and Analysis of Electricity Markets," in *Operation of Market-Oriented Power Systems*, Y.-H. Song and X.-F. Wang, Eds. Springer-Verlag London, 2003.

[88] Z. Wang and K. Lun Lo, "Game Theory Application and Strategic Bidding in the Electricity Supply Market," *World Journal of Engineering and Technology*, 2016.

[89] Y.-H. Song and X.-F. Wang, Eds., *Operation of Market-Oriented Power Systems*. Springer-Verlag London, 2003.

[90] D. J. Gotham, L. Lu, F. W. ad D. G. Nderitu, T. A. Phillips, P. V. Preckel, and M. A. Velastegui, "MISO Independent Load Forecast Update," State Utility Forecasting Group at Purdue University, Tech. Rep., 2017.

[91] "MISO LRZ Annual Energy to Summer/Winter Peak Demand Conversion Factors," 2014, State Utility Forecasting Group at Purdue University. [Online]. Available: https://www.purdue.edu/discoverypark/sufg/docs/publications/2014%20July%20Workshop%20-%20Peak%20Conversion%20Factors.pdf

[92] "PowerWorld Web Help Manual," 2018, PowerWorld Corporation. [Online]. Available: https://www.powerworld.com/WebHelp/

[93] S. Hossain, S. Mohapatra, T. Overbye, and C. Marzinzik, "Automation of commercial power system software for data-driven research," in *2014 Power and Energy Conference at Illinois (PECI)*, Feb 2014, pp. 1–5.